

Computational Analysis of a Membrane-based Separation Process in an Artificial Kidney



By

Ahmed Khan

**School of Chemical and Materials Engineering
National University of Sciences and Technology**

2023

Computational Analysis of a Membrane-based Separation Process in an Artificial Kidney



Ahmed Khan

Reg.No:00000328294

This thesis is submitted as a partial fulfillment of the requirements for the degree of

MS Chemical Engineering

Supervisor Name: Dr. Zaib Jahan

School of Chemical and Materials Engineering (SCME)

National University of Sciences and Technology (NUST)


H-12 Islamabad, Pakistan


August, 2023




THESIS ACCEPTANCE CERTIFICATE

Certified that final copy of MS thesis written by Mr **Ahmed Khan** (Registration No 00000328294), of School of Chemical & Materials Engineering (SCME) has been vetted by undersigned, found complete in all respects as per NUST Statues/Regulations, is free of plagiarism, errors, and mistakes and is accepted as partial fulfillment for award of MS degree. It is further certified that necessary amendments as pointed out by GEC members of the scholar have also been incorporated in the said thesis.

Signature: 
Name of Supervisor: Dr Zaib Jahan
Date: 21/8/23

Signature (HOD): 
Date: 4/9/23

Signature (Dean/Principal): 
Date: 4.9.2023



National University of Sciences & Technology
(NUST)

Form TH-1
(Must be type written)

Final

MASTER'S THESIS WORK

Name: Ahmed Khan
 Department: School of Chemical and Materials Engineering
 Credit Hour Completed: (17) 24
 Formulation of Guidance and Examination Committee (GEC)
 NUST Regn No: 328294
 Specialization: Chemical Engineering
 CGPA: (3.9) 3.75

Course Work Completed

S/No	Code	Title	Core/Elective	CH	Grade
1	EME-921	Momentum, Heat & Mass Transfer In Chemical Engineering	Core	3	B+
2	CHE-853	Green Process Engineering	Elective	3	A
3	RM-898	Research Methodology	Elective	2	Q
4	CHE-843	Separation Processes In Chemical Engineering	Core	3	A
5	CHE-847	Chemical Kinetics & Reactor Design	Core	3	A
6	CHE-814	Product Technology	Elective	3	A
7	ENE-809	Waste Water Treatment & Design	Elective	3	B+
8	ESE-911	Carbon capture & Utilization	Elective	3	B+
9	ENS-830	Cleaner Production Technologies	Elective	3	B+

Date 08/26/2021

Student's Signature *Ahmed Khan*

Thesis Committee

- Name: Dr. Zaib Jahan (supervisor)
Department: School of Chemical & Materials Engineering
- Name: Dr. Muhammad Ahsan (co-supervisor)
Department: School of Chemical & Materials Engineering
- Name: Dr. Muhammad Bilal Khan Niazi
Department: Engineering
- Name: Dr. Noman Ahmed
Department: Engineering

Signature: *Zaib Jahan*

Signature: *Muhammad Ahsan*

Signature: *Muhammad Bilal Khan Niazi*

Signature: *Noman Ahmed*

Date: 20/9/21

Signature of Head of Department: *EB*

APPROVAL

Date: 22-9-2021

Dean/Principal *AG*



National University of Sciences & Technology (NUST)

FORM TH-4

MASTER'S THESIS WORK

We hereby recommend that the dissertation prepared under our supervision by

Regn No & Name: 00000328294 Ahmed Khan

Title: Computational analysis of a membrane-based separation process in an artificial kidney.

Presented on: 24 Aug 2023 at: 1400 hrs in SCME Seminar Hall

Be accepted in partial fulfillment of the requirements for the award of Master of Science degree
in Chemical Engineering.

Guidance & Examination Committee Members

Name: Dr Norman Ahmed

Signature: 

Name: Dr M. Bilal Khan Niazi

Signature: 

Name: Dr Muhammad Ahsan (Co-Supervisor)

Signature: 

Supervisor's Name: Dr Zaib Jahan

Signature: 

Dated: 31/8/23


Head of Department

Date 1/9/23


Dean/Principal

Date 4.9.23

School of Chemical & Materials Engineering (SCME)

Dedication

Dedicated to my extraordinary parents and adored siblings whose marvelous support and cooperation led me to this wonderful accomplishment.

Acknowledgements

I am thankful to Allah Almighty who guided me entire this work. For every step and new thought which You frame-up in my mind to ameliorate it. Indeed, without your priceless help and guidance I could have done nothing. Whosoever helped me throughout the course of my thesis, whether my parents or any other individual was Your will, so indeed none be worthy of praise but You.

I am copiously thankful to my exceptional parents who raised me and continued to support me throughout my Masters.

I would also like to express special thanks to my supervisor Dr. Zaib Jahan for her help throughout my thesis. Who guided and encouraged patronage that I will complete the task of writing and arrangement of the project work well in time.

I would also like to pay special thanks to Dr. Bilal Khan Niazi for his support and cooperation. Each time I got stuck in something, he finds out the solution. I appreciate their patience and guidance throughout the whole thesis.

I would also like to thank Dr. Muhammad Ahsan for being on my thesis guidance and evaluation committee.

Finally, I would like to express my gratitude to all the individuals who have rendered valuable assistance to my study.

Abstract

Patients with kidney failure must undergo long, painful, costly weekly hemodialysis sessions until a donor is found. Reducing the process's time and cost means improving each hemodialysis session's efficiency. Mathematical models are tools used to evaluate the relationship between parameters. Previous models used complex mathematical equations that needed an understanding of various subjects. A user-friendly app is developed using MATLAB R2022 that evaluates parameters, defines their relationship, and makes it convenient to be used by both healthcare professionals and researchers in engineering. The model evaluated the effect of blood flow rate on clearance and predicted that this model had less percentage difference with experimentally measured clearance than previous in-silico models. Also, as the value of the dialysate flow rate increases from 200 mL/min to 1000 mL/min, the percentage difference between the current and previous models reduces at first but then increases at a constant rate. According to the single pool model, drop-in Urea concentration with time is rapid initially but becomes minute towards the end of the session. At a dialysate flow rate of 400 mL/min, the percentage difference between the clearance of the co and counter-current dialyzer is maximum. It starts to decrease as the dialysate flow rate increases. With increasing length and radius of hollow fibers, clearance increases, and the percentage difference between current and previous models' predicted clearance reduces. A rise in residual renal clearance by a value of 0.5 mL/min doubles the standard KT/V , and a similar effect can be seen with an increasing number of weekly dialysis sessions.

Table of Contents

DEDICATION	I
ACKNOWLEDGEMENTS.....	II
ABSTRACT	III
TABLE OF FIGURES.....	VII
LIST OF TABLES	IX
CHAPTER 1.....	1
INTRODUCTION	1
1.1 Background and motivation.....	1
1.2 Problem Statement	5
1.3 Objectives and Scope of the study.....	5
1.4 Research questions	6
1.5 Thesis outline	6
CHAPTER 2.....	7
LITERATURE REVIEW	7
2.1 Overview of Kidney Function	7
2.2 Artificial Kidney Technology	9
2.2.1 Kidney Transplant.....	9
2.2.2 Peritoneal Dialysis	9
2.2.3 Hemodialysis	10
2.3 Membrane-Based Separation Processes	11
2.3.1 Hemodialysis History.....	12

2.3.2 Transport Mechanisms in Membrane.....	12
2.3.3 Diffusion.....	13
2.3.4 Convection.....	14
2.3.5 Osmosis	15
2.3.6 Ultrafiltration	15
2.3.7 Adsorption	16
2.4 Computational Modeling of Membrane-Based Separation Processes.....	16
CHAPTER 3.....	21
Methodology.....	21
3.1 Membrane Module Design	21
3.2 Computational Model Development	22
3.2.1 Change in Urea clearance rate with varying blood and dialysate flow rate	22
3.2.2 Change in Urea concentration with time	23
3.2.3 Effect of flow orientation on Urea clearance.....	24
3.2.4 Effect of overall mass transfer area coefficient on Urea clearance with a varying dialysate flow rate.....	25
3.2.5 Changes in Urea clearance with change in hollow fiber dimensions.....	26
3.2.6 Effect of residual renal clearance on standard and equilibrated hemodialysis adequacy.....	27
3.3 Simulation Scenarios	28
3.3.1 Simulation scenario for change in Urea clearance rate with varying blood and dialysate flow rate.....	28
3.3.2 Simulation scenario for change in Urea concentration with time.....	28
3.3.4 Simulation scenario for the effect of flow orientation on clearance	29
3.3.5 Simulation scenario for the effect of overall mass transfer coefficient.....	30
3.3.6 Simulation scenario for the effect of hollow fiber dimension on clearance	31
3.4 Performance Metrics	32
3.4.1 Mean Squared Error	32

3.4.2 Coefficient of determination.....	32
CHAPTER 4.....	34
Results and Discussion.....	34
4.1 Membrane Module Design Results	34
4.1.1 Change in Urea clearance rate with blood and dialysate flow rate.....	34
4.1.2 Variation in Urea concentration with time during hemodialysis	38
4.1.3 Effect of flow orientation on Urea clearance.....	40
4.1.4 Effect of varying overall mass transfer area coefficient on Urea clearance	42
4.1.5 Changes in Urea clearance with change in hollow fiber dimensions.....	44
4.1.6 Change in values of standard and equilibrated hemodialysis adequacy with increasing residual renal clearance	48
4.2 Discussion of Results.....	50
4.2.1 Validation of the models	50
4.2.2 Mean Square Analysis.....	51
4.2.3 Coefficient of Determination	54
4.3 Sensitivity Analysis.....	55
4.3.1 What is sensitivity analysis?.....	55
Conclusion and Recommendations	57
Summary of Findings	57
Limitations and Future Research Directions	57
REFERENCES	59

Table of Figures

Figure 1 Structure of Nephron (3)	2
Figure 2 Excretory system of the human body (15)	7
Figure 3 Working of Nephron (16).....	8
Figure 4 Structure of the human kidney (17)	8
Figure 5 Process of peritoneal dialysis (24)	10
Figure 6 Process of Hemodialysis (26)	11
Figure 7 Journey of membranes (28)	11
Figure 8 Diffusion process occurring in hemodialysis (34).....	13
Figure 9 Convection phenomena occurring in hemodialysis (37).....	14
Figure 10 Osmosis in dialysis.....	15
Figure 11 Ultrafiltration occurring in hemodialysis (11).....	16
Figure 12 A comparison of the pore diffusion model (left) with the tortuous pore diffusion model (right) (51)	19
Figure 13 Membrane module showing directions of fluid flow	22
Figure 14 User interface of the app to find change in Urea concentration with change in time	29
Figure 15 User interface of the app to calculate the change in clearance with a change in flow orientation.....	30
Figure 16 User interface of the app to calculate the change in Urea clearance with change in overall mass transfer coefficient	31
Figure 17 User interface of the app to calculate the change in Urea clearance with a change in dimensions of the hollow fibers.....	32
Figure 18 Urea clearance values for in-vitro and in-silico scenarios with varying blood flow rate and constant dialysate flow rate ($Q_d=500$ mL/min)	34
Figure 19 Model predicted Urea clearance vs. in silico solute clearances plotted at increasing dialysate flow rate at $Q_b=400$ mL/min.....	37
Figure 20 Graph showing the decrease in Urea concentration over time	39
Figure 21 Difference in Urea clearance with change in flow orientation at different dialysate flow rates	41

Figure 22 Effect of overall mass transfer area coefficient on clearance with changing dialysate flow rates43

Figure 23 Change in Urea clearance rate with change in length of hollow dialyzer fiber 45

Figure 24 Change in Urea clearance rate with change in radius of hollow fiber47

Figure 25 Change in std KT/V with increasing residual renal function at different numbers of hemodialysis sessions per week49

List of Tables

Table 1 Classification of Glomerulus filtration rate	3
Table 2 Classification of Uremic toxins in blood (9)	4
Table 3 Values of parameters used for Urea clearance vs. Qb model	23
Table 4 Values of parameters used for Urea clearance vs Qd model	23
Table 5 Values of parameters used for Urea concentration vs. Time model	24
Table 6 Values of parameters used for finding Urea clearance in Co and Counter current flow arrangement	25
Table 7 Values of parameters used for evaluating the effect of overall mass transfer area coefficient on Urea clearance	26
Table 8 Values of parameters for evaluating change in Urea clearance with change in hollow fiber dimensions	27
Table 9 Values of parameters for evaluating the effect of residual clearance on standard and equilibrated hemodialysis adequacy	28
Table 10 Comparison of model results with the literature (55, 58, 66)	35
Table 11 Percentage difference between this model and previous models (55, 66).....	37
Table 12 Change in Urea concertation with time	39
Table 13 Percentage difference in clearance rate with increasing dialysate flow rates for Co and Counter current flow arrangements	41
Table 14 Percentage difference in clearance of dialyzers with low and high overall mass transfer area coefficient	43
Table 15 Percentage difference between models showing a change in Urea clearance with a change in length of fiber	45
Table 16 Percentage difference between models showing a change in Urea clearance with a change in the radius of a fiber	47
Table 17 Increase in std KT/V with an increase in the number of hemodialysis sessions per week	49
Table 18 Table showing Mean square error for model calculating clearance w.r.t dialysate flow rate	52
Table 19 Table showing Mean square error for model calculating clearance w.r.t hollow fiber length	52

Table 20 Table showing Mean square error for model calculating clearance w.r.t hollow fiber radius.....53

Table 21 Table showing R square values for the model predicting the clearance w.r.t dialysate flow rate.....54

Table 22 Two variable sensitivity analysis showing a change in clearance with changing length and dialysate flow rates55

Table 23 Two variable sensitivity analysis showing a change in clearance with changing radius and dialysate flow rates56

Chapter 1

Introduction

1.1 Background and motivation

Kidneys are bean-shaped structures located beneath the ribcage in the human body. They are responsible for filtering the blood, thus keeping the concentration of nutrients at an average level. A common problem with the kidney is its failure which occurs when the filtration rate of the kidney falls below $16 \text{ mL}\cdot\text{min}^{-1}$ [1]. In this case, the toxins in the blood do not get filtered out properly, and their concentration starts to build up, which can lead to life-threatening circumstances.

The weight of kidneys in human males is 125-170 g and 115-155 g in women; the latter have elongated size of kidneys. The kidney's central functional unit is the Nephron; each kidney has around a million nephrons. Inside the nephron is a glomerulus surrounded by a network of capillaries called the Bowman's capsule [2]. The walls of these capillaries are made of micro voids which filter toxic wastes from blood by a difference in pressure. Figure 1 shows a detailed structure of a nephron.

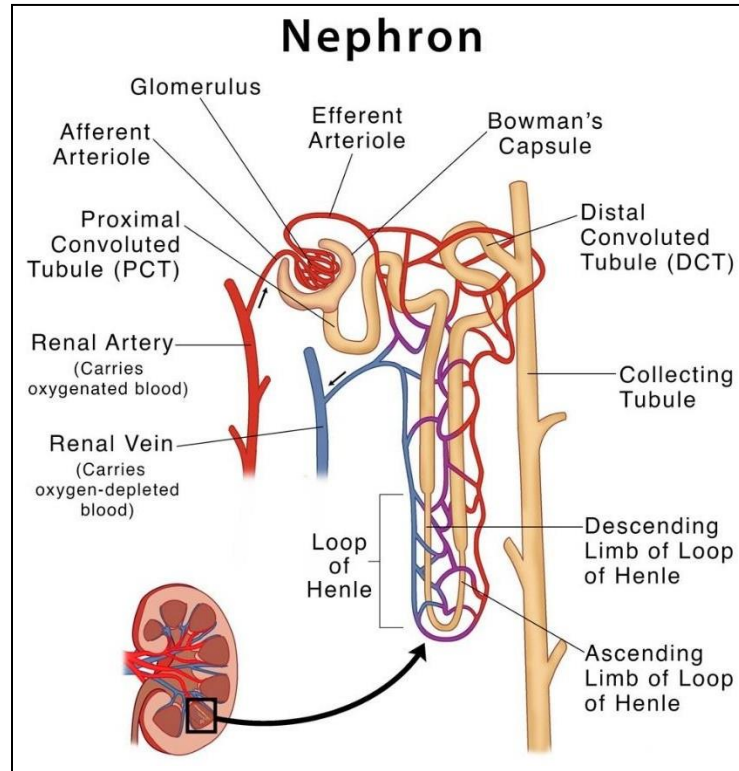


Figure 1 Structure of Nephron [3]

Along with filtering the blood, the kidney has other vital functions within the human body, such as [4]:

- It maintains the acid-base levels of the human body.
- It is responsible for hormones such as erythropoietin, which protects red blood cells from destruction.
- The kidneys are responsible for converting vitamin D obtained from supplements to the active form required by the body.

Kidney or renal failure is when one or both kidneys cannot function correctly, i.e., they cannot remove uremic toxins from the blood.

Two common types of renal failure include Chronic Renal Failure (CRF) and Acute Kidney Injury (AKI). In AKI, sudden damage to the kidneys happens over a few days or months and is commonly caused due to low blood volume after bleeding, excessive vomiting, and severe dehydration [5].

In CRF, the filtration rate of the renal capsule falls below 60ml/min/1.73m² of the body's surface area for a minimum of three months. Consequently, urine output is less than 0.5 ml/kg/hr for more than six hours, and creatinine level is equal to or more than 0.3 mg/dL [6]. Table 1 shows a classification of CRD.

Table 1 Classification of Glomerulus filtration rate

Description	Glomerulus filtration rate (GFR) (mL/min/1.73m ²)
Normal function	≥90
Mildly decreased functioning	60 to 89
Moderately decreased to mildly decreased	45 to 59
Moderately to severely decreased	30 to 44
Severely decreased	15 to 29
Kidney failure	<15

As a result of renal failure, the concentration of uremic toxins starts building up in the blood to a life-threatening level. Uremic toxins are molecules produced due to various reactions in the human body and are classified into three categories.

- Water soluble toxins
- Protein-bound toxins
- Large toxins

Water soluble uremic toxins are those toxins that have a molecular weight of less than 500 Da, such as Urea and Creatinine. They only dissolve in water and do not get bound to protein. Hence they are relatively easier to remove from blood [7].

Protein-bound toxins get attached to the albumin present in the blood. Albumin is a protein present in blood that is responsible for not letting fluids in blood leak into other tissues. It is also responsible for carrying enzymes and hormones through the human body. Protein-

bound enzymes attach to albumin; common examples are p-cresol and indoxyl sulfate. These compounds are responsible for chronic kidney diseases and can lead to kidney failure over a longer time [8].

The large toxins category includes those with a molecular weight greater than 500 Da, for example, β 2-microglobulin.

Table 2 is a tabular representation of toxin categories found in the blood.

Table 2 Classification of Uremic toxins in blood [9]

Type of toxin	Weight (gmoI ⁻¹)	Toxins
Water soluble toxins	60	Urea
	168	Uric acid
	113	Creatinine
Protein-bound toxins	108	p-cresol
	251	Indoxyl sulfate
Large toxins	>500 Da	β 2-microglobulin

Typical drivers for kidney failure include diabetes, hypertension, obesity, glomerulonephritis (inflammation) or pyelonephritis (infections), enlarged prostate, and long-term use of pain-relieving analgesics. The leading cause is diabetes, a common symptom in one-third of all cases [10]. In Pakistan, the per year average cost of dialysis for a single patient is around 8 to 8.5 lacs which is many times higher than the per capita income of a citizen. Although philanthropists fund several of these patients, many suffer the expense themselves. Most of the patients have to undergo the painstaking process of dialysis twice a week; each session lasts around 4 hours [11]. A more efficient membrane can lead to a reduction in the time of the process. Also, local designing and manufacturing of membranes can lead to reduced cost of membranes, ultimately resulting in reduced cost of the hemodialysis process. Around 17 million people suffer from renal disease of various kinds. The costs associated with dialysis are expected to rise due to inflation in the country [12]. Therefore, there is an urgent need for local designing, manufacturing, and optimizing membrane performance parameters.

Kidney failure leads to the build-up of Urea, and Urea, although itself is mildly toxic. However, its buildup represents that there has been an accumulation of toxins within the human body [13]. Since Urea is a low molecular weight toxin, diffusion removes it from the human body. In contrast, for higher molecular weight toxins such as β 2-microglobulin and complement factor D, convection is the principal phenomenon behind its removal from the human body. The efficiency and the extent of removal of both small and large-size toxins depend upon various parameters related to the hemodialysis process, such as the geometry of hollow fibers, membrane characteristics, and the operating variables [14]. Significant challenges related to the hemodialysis process include the cost and longer times, which can be tackled to some extent with a thorough understanding of the process parameters and their interaction and dependence upon each other. A better understanding and comprehension of process parameters can help design the dialyzer and the hemodialysis process as a whole, to conclude in less time and cost with the least painful side-effects.

1.2 Problem Statement

The hemodialysis membrane simulations have been performed using COMSOL Multiphysics using computational fluid dynamics concepts, but these concepts require extensive background knowledge. Therefore, a more straightforward approach is needed to perform simulations and understand the relations between process parameters. Also, there is a need for a user-friendly app that allows physicians and researchers to analyze the effects of various parameters on each other for the prognosis of the condition. The current work is focused on simulating and analyzing the interaction between various process parameters related to hemodialysis, investigating the underlying causes behind each trend and relation of parameters, and finally developing a user-friendly app that can assist in understanding the effect of various parameters.

1.3 Objectives and Scope of the study

The study aims to investigate the relationship between changes in concentration of Urea with varying blood and dialysate flow rate, the change occurring in Urea concentration overtime during the hemodialysis process, the influence of flow orientation on the clearance of Urea during hemodialysis, the effect of overall mass transfer area coefficient

on clearance of Urea, variation in Urea clearance with changing dimensions of hollow fiber and finally the relationship between hemodialysis adequacy and residual renal clearance. MATLAB 2022b was used to develop the simulations and app. MATLAB comes with a built-in app developer that was utilized for developing the app.

1.4 Research questions

Regarding hemodialysis challenges, cost and time outweigh all other process concerns since the patients have to undergo painful procedures several times weekly. The cost of the process and equipment required is another pain point. The primary concern of physicians in the hemodialysis process is to eliminate as many toxins as possible while retaining the valuable components in blood. Therefore, clearance, a significant indicator of process efficiency and adequacy, must be explored thoroughly. Research is focused on what values of process parameters provide us with optimal efficiency and where exactly we need to set values for parameters to optimize the cost of the process. Increasing the values of parameters comes with a specifically associated cost that needs to be paid by the patient. Therefore, optimal values required for clearance are needed while minimizing the cost of the process.

1.5 Thesis outline

The introductory chapter discusses the background of the problem, the current study's objectives, and the research questions that are investigated. Chapter 2 contains a literature review of the problem at hand, a thorough understanding of the underlying phenomena occurring, and the previous research that has been conducted related to the topic. Chapter 3 focuses on the simulation and app developing part of the research and thoroughly discusses the software, equations, and assumptions involved. Chapter 4 contains the results of simulations and the final images of the app that has been developed, while final chapter 5 contains the conclusions and the discussion.

Chapter 2

Literature review

2.1 Overview of Kidney Function

The excretory system is responsible for removing the toxins built up in the human body. Kidneys are a vital organ of this system, responsible for excreting the wastes that build up in the human body and removing extra minerals to maintain an equilibrium of water and salts. Also, kidneys are responsible for hormones that control blood pressure, making red blood cells and hormones to keep bones strong and healthy.

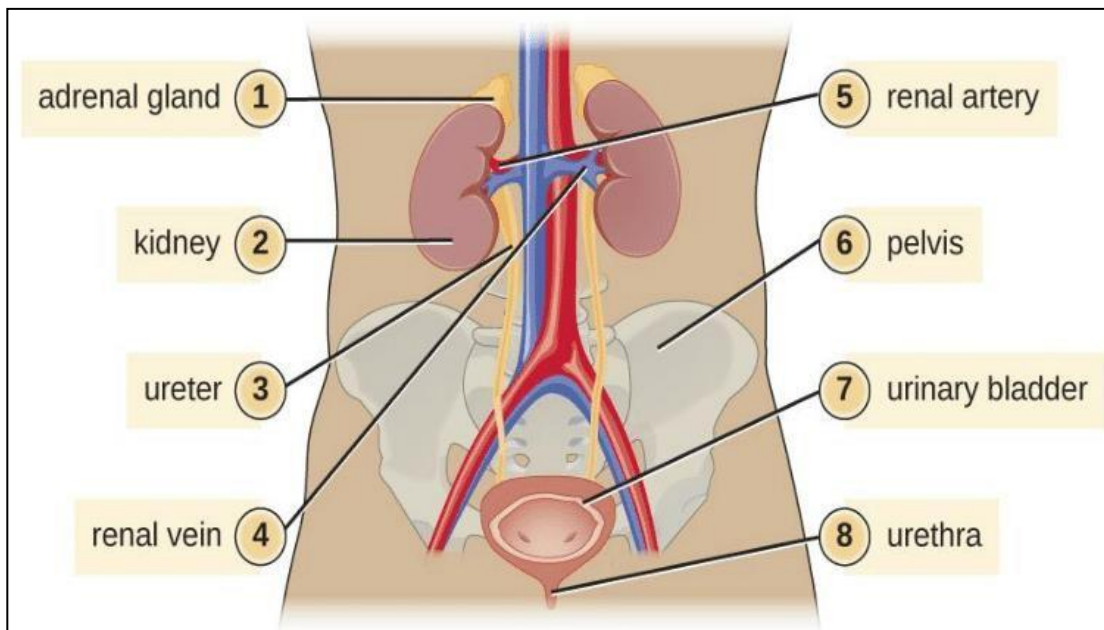


Figure 2 Excretory system of the human body [15]

When it comes to filtering blood, the primary component within the kidney that is responsible for filtering wastes is the nephron. Each kidney has around a million nephrons containing a glomerulus filter and a tube known as a tubule. The blood enters the nephron through the renal artery and passes through the glomerulus. Glomerulus then extends further and wraps around a large tube called the tubule which returns those essential substances needed to the human body to the body. The renal vein then takes the remaining wastes towards excretion from the body.

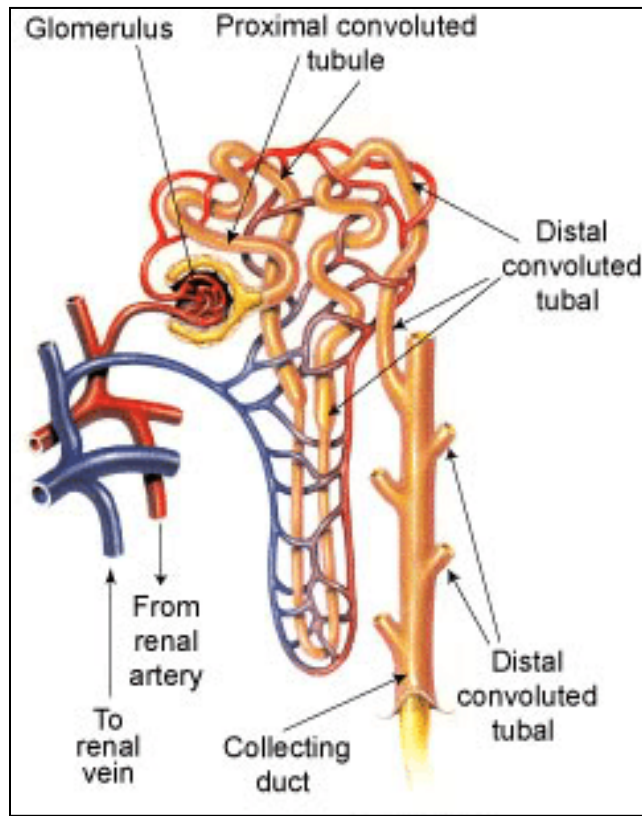


Figure 3 Working of Nephron [16]

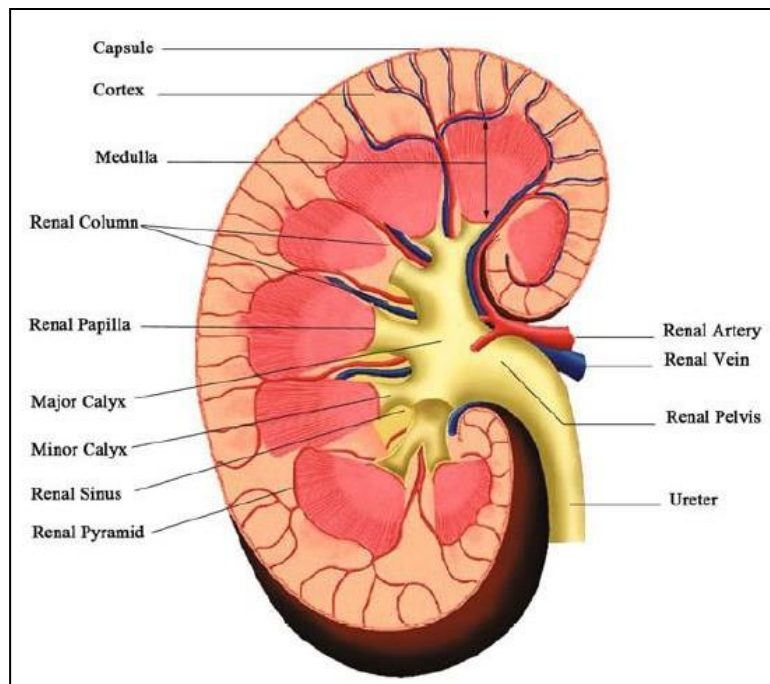


Figure 4 Structure of the human kidney [17]

Kidneys remove Uremic toxins from the body produced due to various reactions in the human body. The Urea cycle occurring in the liver is the primary reaction responsible for producing Uremic wastes.

2.2 Artificial Kidney Technology

The mortality rate due to chronic kidney disease is reported to be around 15% in the Western world, which is similar to the percentage of colon cancer [18]. Kidney failure treatment is the process of Dialysis and is performed using an artificial kidney or a Dialyzer. A dialyzer removes excess salts, fluids, and toxins from the patient's blood. The dialysis process has proved to be a successful substitute to donor nephrectomy in which a healthy person's kidney is removed and installed into a patient suffering from kidney failure [19]. However, other substitutes to hemodialysis are peritoneal dialysis and kidney transplant, which are discussed as follows:

2.2.1 Kidney Transplant

Kidney transplant is one of the solutions employed to treat End Stage Renal Disease (ESRD), in which the defected kidney of a patient is replaced with a healthy one. It is a surgical process and requires a consensual donor to donate his or her kidney. The surgery is followed by a long period of extreme care, as even a single infection can lead to the failure of the process [20]. Rejection is a common observation in such cases where the body refuses a foreign kidney. The immune system treats the donated kidney as a foreign object and attacks it. Medication ensures that the immune system does not damage the newly planted kidney in the patient [21]. Also, the donor has to be in good health and should be a good match with the receiver's body. Along with health risks and the cost of kidneys, the surgery itself is very costly, and in third-world countries, people find it challenging to go for this treatment for end-stage renal disease.

2.2.2 Peritoneal Dialysis

Peritoneum is a serous membrane inside the abdomen that forms the lining of the abdominal cavity and covers the organs in the abdomen. In peritoneal dialysis, a solution mainly consisting of water, salt, and other additives is introduced outside the peritoneum. The patient can move around and perform daily life activities after fluid insertion [22]. After a specific time, the fluid absorbs the wastes in the blood, and the used fluid is

discarded. Disposed fluid is replaced with a new one, repeated four to six times daily. Common problems associated with peritoneal dialysis include Hernia and infections [23]. Also, weight gain is a common complaint from patients undergoing peritoneal dialysis. Figure 4 shows the process of peritoneal dialysis.

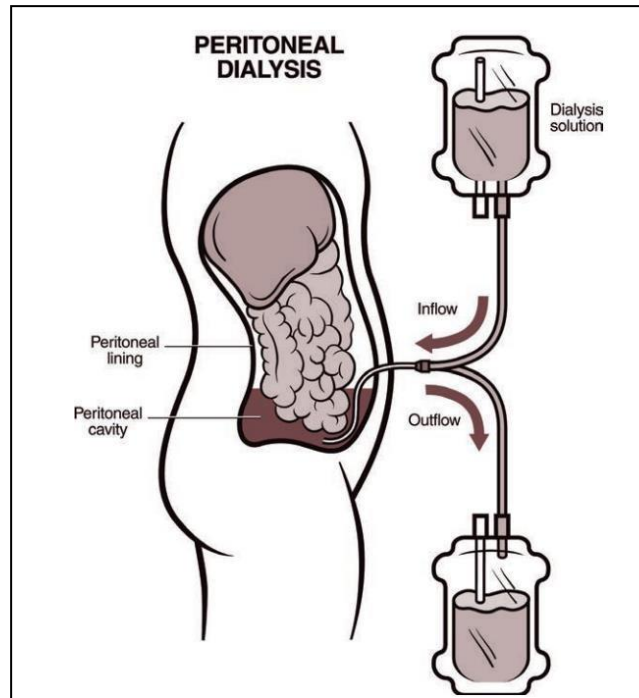


Figure 5 Process of peritoneal dialysis [24]

2.2.3 Hemodialysis

In this type of dialysis, a device called a dialyzer is used, which contains membranes that purify the blood. A dialysate solution is made to flow on one side of the membrane, while on the other side, blood is made to flow. The toxins in blood move to dialysate through the mechanism of convection, diffusion or ultrafiltration and purified blood is injected back into the patient's body [25]. The temperature and blood pressure are essential parameters maintained throughout the process. Heparin is an anti-coagulant used to prevent the formation of blood clots during the process. The dialysate is continuously changed to maintain a constant concentration of minerals in it. The hemodialysis process lasts about four hours and is done three to six times per week, depending upon the severity of the case [26]. Figure 5 shows the process of hemodialysis.

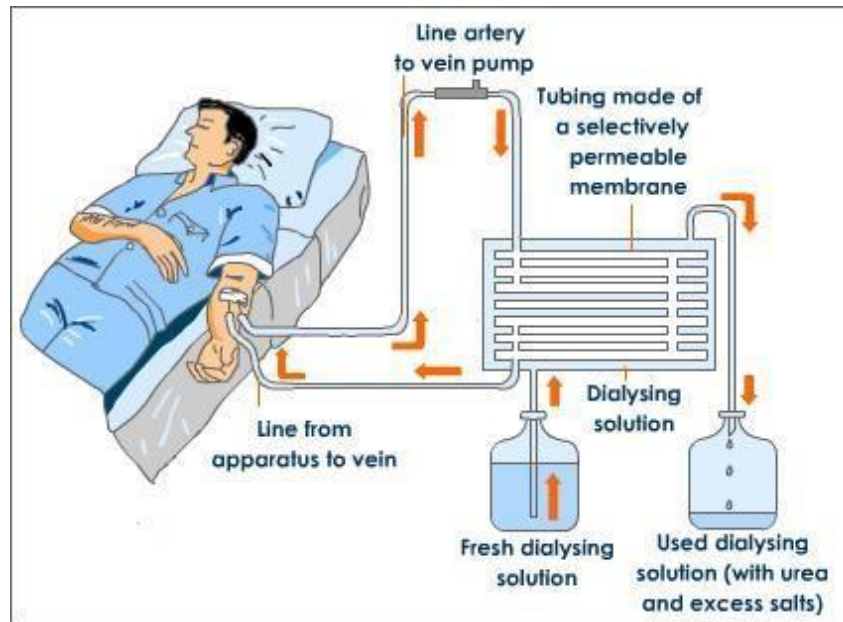


Figure 6 Process of Hemodialysis [26]

2.3 Membrane-Based Separation Processes

The membrane-based separation process in hemodialysis occurs inside the membrane of the dialyzer. Besides being used for hemodialysis, membrane technology has lucrative applications in several other fields, such as water purification, the separation of gases and chemicals, the beverage industry, and biomedical fields. During World War II, this technology gained profound interest, especially for cleaning water and in the biomedical engineering realm [27]. The idea of using membranes as a semipermeable barrier has been under discussion since the early 1900s. Figure 6 shows a summarized history of the journey which membranes have gone through since their invention.

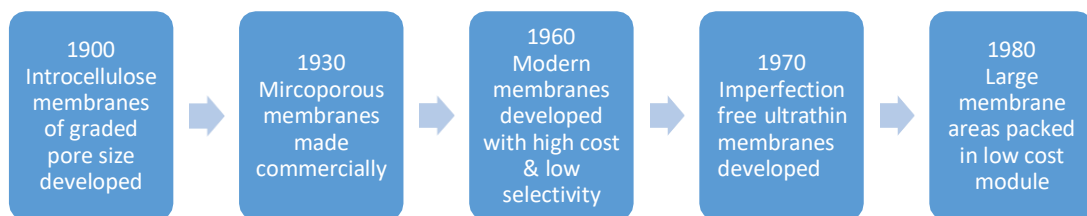


Figure 7 Journey of membranes [28]

Since 1971, the use of membrane separation technology has been on the rise, and currently, the membrane industry's worth stands at US\$1-2 billion per year.

2.3.1 Hemodialysis History

Prof. Abel performed the first dialysis using a celloidin tube in Philadelphia. He investigated the separation process of two fluids passing through these tubes. Later, Prof. Alwall, in an experiment, showed that cleaning of blood could also be done using an artificial kidney around 30 years ago. The work done by the latter paved the path for the modern day hemodialysis process that we utilize. After several modifications and improvements in his work, today we have modern dialysis that is highly efficient and lifesaving [29, 30]. The first artificial kidney center was developed by James Haviland and Scribner in 1962, and it was also the first nonprofit kidney disease treatment center where their most significant challenge was to enhance and improve the efficiency of hemodialysis technique so that it is cost-effective, cheap, and has less mortality rate [31]. Despite the efforts of researchers, a few challenges that remained persistent throughout hemodialysis' inception were the accumulation of toxic large and middle-size molecules. To this day, the efficient separation of middle molecules remains an area of deep interest for all researchers [32].

The efficiency and outcome of the membrane separation process depend highly on the membrane, which is the heart of the entire process. Once the pressure is applied, it allows specific molecules to pass through it while retaining the others based on certain factors such as the membrane's selectivity, size of pores, the affinity of molecules towards the membrane, and physiochemical reactions occurring at the membrane's surface. The stream of liquid fed to the membrane is referred to as the feed stream, and the stream that successfully passes through the membrane is referred to as permeate. In contrast, those species retained by the membrane during hemodialysis are called retentate or the retained constituents [33].

2.3.2 Transport Mechanisms in Membrane

In hemodialysis, blood and dialysate are made to come into contact with each other through a semi-permeable hollow fiber membrane. During this contact, toxins in blood move from the blood to dialysate while the ions in dialysate move from dialysate to the

blood side, thus replicating the auctioning of kidneys present in the human body. Diffusion and convection are prominent mechanisms during this bi-directional flow process of molecules and ions. Alongside diffusion and convection, ultrafiltration, osmosis, and adsorption are also at work.

2.3.3 Diffusion

Diffusion is defined as the process during which the molecules of a species move from a region of higher concentration to a region of lower concentration by the Brownian motion. The driving force involved in diffusion is the concentration difference between the two regions [34]. As shown in the Figure 8, the metabolic toxins in the blood stream move from the region of their high concentration (blood) to the low concentration side (dialysate). At the same time, the movement of electrolytes such as Sodium and Magnesium occurs from dialysate side to the blood stream.

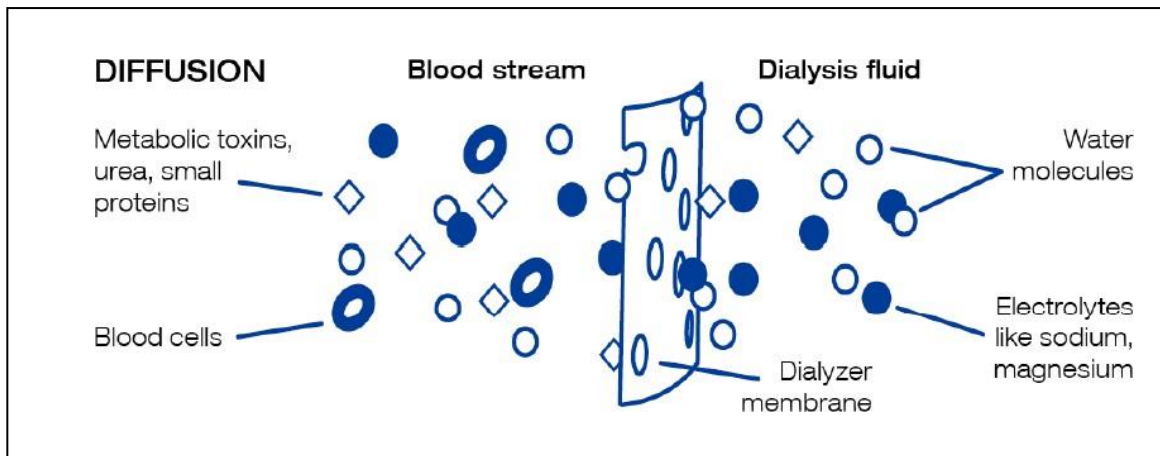


Figure 8 Diffusion process occurring in hemodialysis [34]

The diffusion process in hemodialysis depends upon the blood and dialysate stream concentration, their flow rates, the temperature of the fluids, viscosity, and morphology or surface area of the membrane. Of all the mentioned variables, one that is decisive is the difference in concentration of both fluid streams [35]. The governing equation used to describe diffusion phenomena is called Fick's law.

$$J = -cD \left(\frac{\partial c}{\partial x} \right) \quad (1)$$

In Eq. (1) the rate of diffusion flux is represented by J and has units of $\text{m}^{-2}\text{s}^{-1}$, diffusion coefficient D has units of m^2s^{-1} , while c represents the molar density and has units of $\text{kmol}\cdot\text{m}^{-3}$. The concentration gradient is represented by the partial differentials of c and x where concentration units are gm^{-3} and distance is m^{-2} .

2.3.4 Convection

The driving force for diffusion is the concentration gradient, while for convection, the driving force is the pressure gradient. The transport of middle-sized molecules from the blood to the dialysate stream occurs through convection. The significant variables determining the extent of convection in hemodialysis are hydraulic permeability, sieving coefficient, membrane area, and, most importantly, the pressure gradient applied across the membrane [36]. Figure 9 shows the phenomena of convection occurring during hemodialysis.

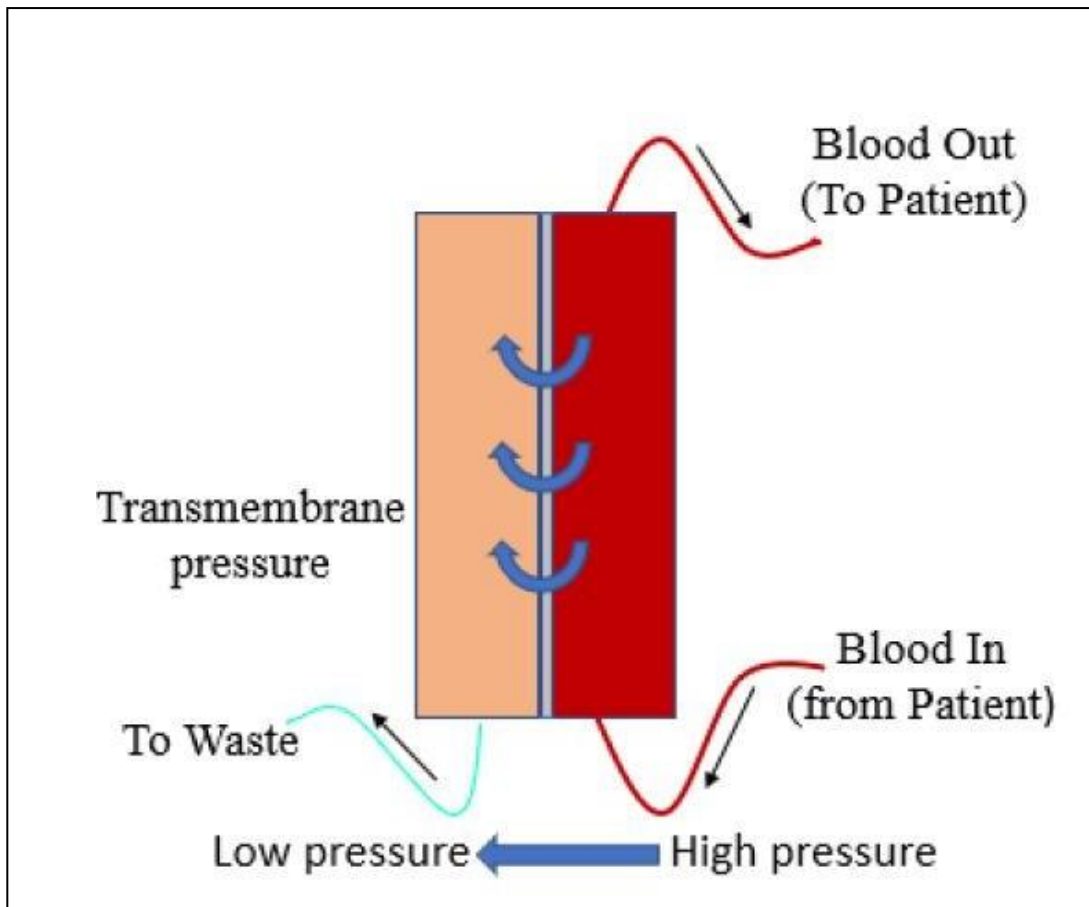


Figure 9 Convection phenomena occurring in hemodialysis [37]

2.3.5 Osmosis

The process of Osmosis, like diffusion, depends upon the difference in concentration on both sides of the membrane. However, unlike diffusion, where molecules move from a region of high to low concentration, in osmosis, molecules move across a semi-permeable membrane from a region of low to a region of high concentration. During hemodialysis, osmosis is responsible for water movement across a membrane into the blood [38]. Figure 10 illustrates the phenomena of osmosis occurring in dialysis.

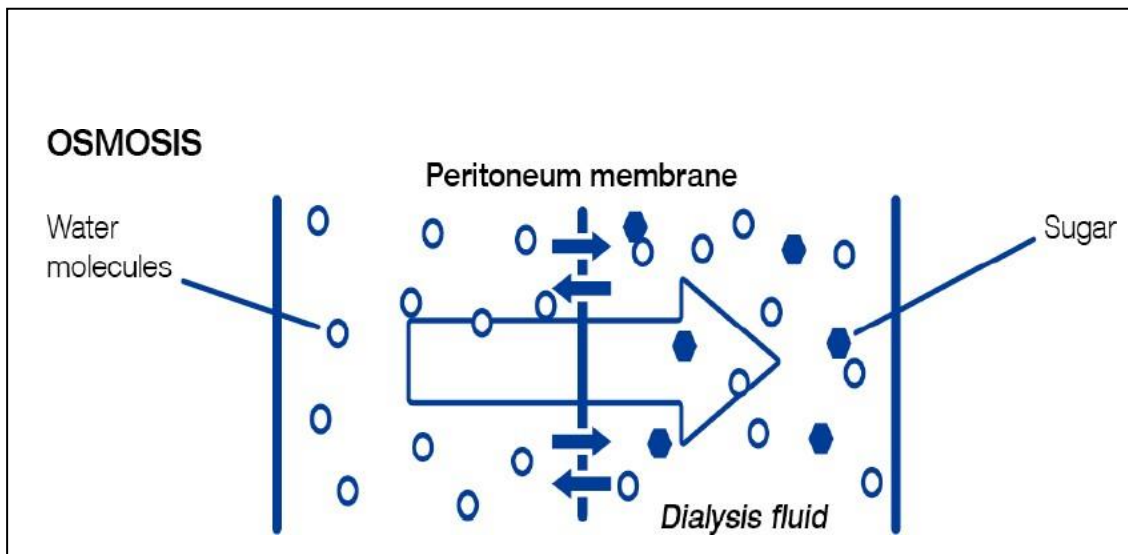


Figure 10 Osmosis in dialysis

2.3.6 Ultrafiltration

The ultrafiltration process is the one through which excess water is removed from the body when it moves from blood to dialysate due to pressure differences. The blood side has a higher pressure than the dialysate side, so the water starts moving from the high to the low-pressure side [39]. The ultrafiltration process depends on variables such as blood pressure and the porosity of the membrane across which transfer is occurring. It is also responsible for removal of middle-sized toxin molecules.

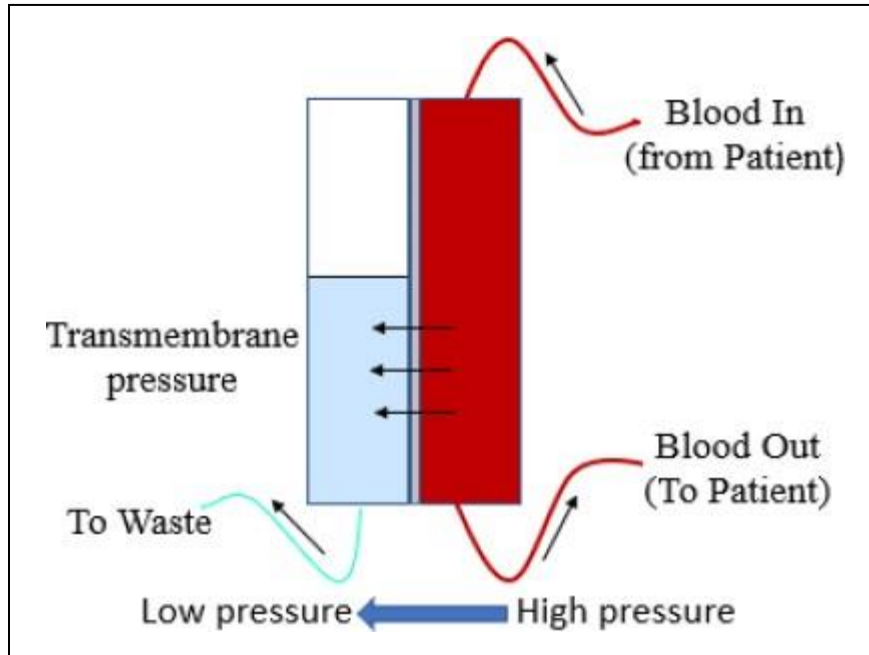


Figure 11 Ultrafiltration occurring in hemodialysis [11]

2.3.7 Adsorption

Adsorption is a phenomenon that occurs during hemodialysis when the molecules present in the blood stream start forming blonds at the surface of the membrane. A specific class of toxins exhibits such behavior as P-cresol, peptides, and indoxyl-sulfate [40]. Such molecules are eliminated from the blood stream either by attaching themselves to the membrane surface or the adsorbent in the membrane. Few proteins that are adsorbed on the surface and need to be introduced back into the blood stream are retained in the blood through back flushing.

The extent to which adsorption occurs depends upon the surface area of the membrane since this phenomenon occurs on the membrane [41].

2.4 Computational Modeling of Membrane-Based Separation Processes

For the first time, Zydney AL used simulations and modeling to understand the convective and bulk transports occurring across the hollow fibers. He deduced that convective transport occurring across the membrane plays a vital part in defining and improving the clearance efficiency of membranes used for hemodialysis. His work also resulted in the formation of model equations for dialysate and blood side compartments and for both diffusive and convective transport across membranes [42].

Jaffrin MY developed an empirical relation for finding out the total clearance that included both the effects of convective and diffusive transport across the membrane, and this relation is as follows:

$$K = K_D + 0.4Q_f + 8.3 \times 10^{-3}Q_f \quad (2)$$

In the Eq. (2), Q_f is the flow rate of ultrafiltration. The work discusses three models that calculate clearance using a concentration of toxins at the outlet and sieving coefficient. The outcomes and results found using the above relation were in satisfactory agreement with the works of other authors who performed simulation-based work [43].

A theoretical model developed by Legallais C showed the effect of design parameters, membrane characters, and process parameters on clearance efficiency. A model developed by Legallais C incorporated the influence of concentration polarization, change in mass transfer coefficient for flow rate, and variations in water flux in the module. The model showed that if saline and plasma were substituted with blood, there was an agreement of 10% and 20% with in-vivo results, respectively [44].

A mathematical model was developed by Coli et al. for evaluating the body fluids and solutes transport in hemodialysis. The study proposed a 3-compartment model for fluid transport while a 2-dimensional model was presented for solute transport. For validating the simulations, in-vivo clinical data was used. The results showed a change in ultrafiltration profiles with time and changes in concentrations for solutes such as Urea, Sodium, and Potassium. These results agree with the data obtained from patients [45].

During hemodialysis, small-sized molecules are transported via diffusion, while for middle-sized molecules, the dominant phenomenon is ultrafiltration across the membrane [46]. Many research articles used the following equations to find out the flux of solutes and the flux of ultrafiltration.

$$J_V = L_p(P_B - P_D - \Delta\pi) \quad (3)$$

$$J_S = K_O(C_B - C_D) + J_V\gamma(f_B C_B + f_D C_D) \quad (4)$$

In the Eq. (3) and Eq. (4), J_V and J_S represent fluxes of ultrafiltration of solutes, respectively, while γ shows the value of the sieving coefficient, which varies between 1

to 0. In the case of Urea, the value of the sieving coefficient is taken as 1, while for larger particles, it is taken as less than 1. L_p represents hydraulic permeability multiplied by osmotic and oncotic pressure differences. CB and CD represent the concentration of dialysate and blood compartment.

A comparison of models presented by Legallais, Waniewski, and Jaffrin was done by Galach M et al. and found that all these models are 1-dimensional and utilize simple assumptions to find the value of mass transfer coefficient across the dialysis membrane [46]. The model of Legallais utilizes individual mass transfer coefficients at the membrane and inside the membrane [44, 46]. The model presented by Waniewski combines the overall mass transfer coefficient with the membrane's permeability [46]. Jaffrin found the empirical relations that evaluate the dependence of the coefficient of transmittance on flow rates of ultrafiltration [47].

Finite Element Analysis (FEA) was performed by Conrat et al. on the hollow fibers with hexagonal geometry. He applied continuity and mass transport equations for convection-diffusion with the Navier-Stokes equation to determine the momentum [48]. Merrill equation found the effect of concentration polarization on osmotic pressure and boundary layer [43]. Incorporating the Brinkman equation with porous media, considering blood as non-Newtonian fluid, and including the Carreau-Gambarodo model, the non-Newtonian behavior of blood was observed [49].

A virtual patient model developed by Galach M et al. showed the physiological processes occurring during hemodialysis. It helped select dialysis treatment for a particular patient profile. The work done by Galach showed variations in glucose levels and volume changes with time while the process of peritoneal and hemodialysis [50].

“Tortuous Capillary Pore Diffusion Model (TCPDM)” was presented by Yammamoto K et al., which provided a better water flux and permeability estimation than a simple pore diffusion model. With the incorporation of tortuosity, the path length for diffusion is longer compared to straight, right-angle displacements [51].

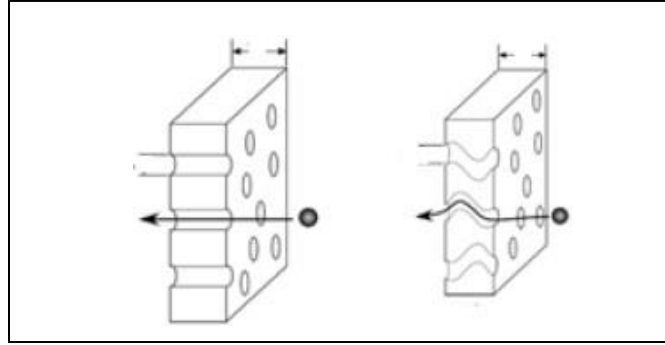


Figure 12 A comparison of the pore diffusion model (left) with the tortuous pore diffusion model (right) [51]

A study by Azar et al. showed that dialyzer clearance and Urea reduction ratio could be enhanced by increasing the dialysate flow rates. It was proved through an in-vivo study done on 138 patients undergoing dialysis [52].

The model presented by Olson JC introduced the design of the portable system of hemodialysis. In this work, Simulink was utilized to design the model in which several inputs were provided, including the dialyzer's geometry, therapy time, and blood flow rate. This model was validated using in-vitro experimental results obtained using porcine blood and other published data from hemodialysis patients [53].

A computational analysis was performed by Lu J. et al. of flow through parallel paths of channels in which the Kende-Katchalsky model and Navier Stokes equations were simulated to form the concentration distribution profile and velocity field.

Shihamul Islam studied the commercially available dialyzer membrane named Polyflux 210H, in which the manufacturer provides process and design parameters [54]. Field emission scanning Electron microscopy was used to examine and study the membrane's morphological aspects. The author applied the pore diffusion model using COMSOL Multiphysics 4.3 to simulate a mathematical mode of the membrane [55]. The work did not include the effect of tortuosity. However, it plays a massive role in the clearance of middle and big-sized molecules as giant molecules face considerable hindrance by a zig-zag path rather than a straight one.

Ding W et al. used COMSOL Multiphysics to form the geometry and simulation of the dialyzer. They also developed the 3D geometry, including housing, dialysate, blood inlets,

outlets, and hollow fibers. The simulation showed that the clearance rate could be increased by increasing the flow rate of blood and dialysate [56].

Ravagli E et al. developed an updated mathematical model of hollow fibers by connecting it with the blood pool model. As a result, the model can update the change in blood concentration with time [57].

Using the COMSOL Multiphysics Finite element method (FEM), Donato D et al. has shown the effect of the aspect ratio of hollow fibers, pressure across membrane module, and packing density of module on the overall clearance efficiency for different solutes [58].

Chapter 3

Methodology

3.1 Membrane Module Design

A membrane module comprises a collection of hollow fibers bundled together, as Figure 13 shows. In a commercially available membrane module, around 12000 hollow fibers are present inside a shell enclosed by a covering. There are two inlets and two outlets for both the fluids, and the blood flows through the cavity of hollow fibers, while dialysate is made to flow through the annular space between fibers and the external shell. Due to convection and diffusion occurring between the two fluids, the purification of blood takes place while, at the same time, electrolytes present in the dialysate move into the blood to balance the electrolytes in the bloodstream. In contrast, modeling in most instances is assumed that the fibers are uniformly spaced in a hexagonal order, and the spaces between the annulus are neglected. It must also be noted that in case of uneven spacing between the fibers, the overall mass transfer coefficient value is reduced, thus reducing the efficiency of the dialyzer. Also, the flow orientation inside the dialyzer is kept countercurrent to maximize the concentration gradient throughout the length of the dialyzer as fresh dialysate comes in contact with blood moving towards the dialyzer outlet. For this study, Urea was the toxin under consideration for all models, although it is mildly toxic. However, its high levels indicate other toxins also build up within the body. Also, most of the nitrogenous wastes from the human body are eliminated in the form of Urea. It is produced in the human body through the Urea cycle, mainly in the liver but also to some extent in other body tissues [59].

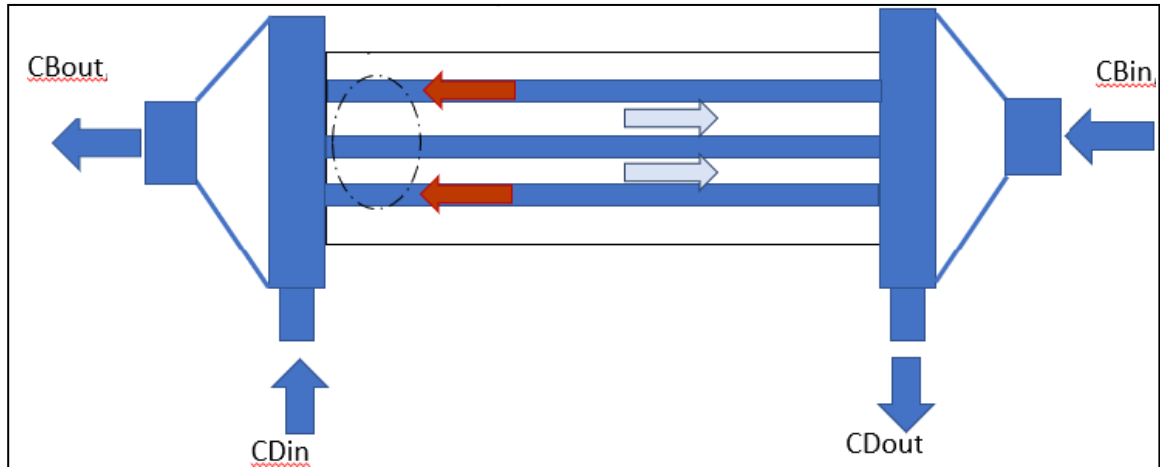


Figure 13 Membrane module showing directions of fluid flow

3.2 Computational Model Development

Different computational models were developed using relevant equations and assumptions. The following is a list of models that were first developed in MATLAB and then were further transformed using MATLAB app designer in the form of an app.

- Change in Urea clearance rate with blood and dialysate flow rate
- Change in Urea concentration with time
- Effect of flow direction on Urea clearance with a varying dialysate flow rate
- Effect of overall mass transfer area coefficient on Urea clearance with a varying dialysate flow rate
- Changes in Urea clearance with changes in hollow fiber dimensions
- Effect of residual renal clearance on standard and equilibrated hemodialysis adequacy

The following section discusses the development of models individually.

3.2.1 Change in Urea clearance rate with varying blood and dialysate flow rate

For finding the change in clearance of Urea with varying values of blood flow rates, Eq. (5) was used:

$$Kd = QbQd \frac{\frac{KA}{Qd} - \frac{KA}{Qb}}{Qd e^{\frac{KA}{Qb}} - Qb e^{\frac{KA}{Qd}}} \quad (5)$$

Qd is dialysate, and Qb is blood flow rate; both are in mL/min. Kd is the value of clearance in units of mL/min. The value for dialysate flow rate was kept constant at 500 mL/min while the value of blood flow rate was initially kept at 300 mL/min and later at 400 mL/min. The results were compared with experimental data and in-silico findings of Islam et al. and Tooba et al. The value of KoA was kept to 1000 mL/min to assume a high-efficiency dialyzer. Table 3 summarizes the values used to develop a model.

Table 3 Values of parameters used for Urea clearance vs. Qb model

Parameter	Value	Units
Overall mass transfer coefficient, KoA	1000	mL/min
Dialysate flow rate, Qd	500	mL/min
Blood flow rate, Qb	300,400	mL/min

Eq. (5) was used to find the change in Urea clearance rate with increasing dialysate flow rate. The value of the dialysate flow rate varied from 200 mL/min to 1000 mL/min, and the resulting plot was compared with previous in silico investigations. The value of the parameters was as per Table 4:

Table 4 Values of parameters used for Urea clearance vs Qd model

Parameter	Value	Units
Overall mass transfer coefficient, KoA	1000	mL/min
Blood flow rate, Qb	400	mL/min
Dialysate flow rate, Qd	200-1000	mL/min

3.2.2 Change in Urea concentration with time

The following Eq. (6) is used to find the change in the concentration of Urea over time.

$$C_e(t) = C_0 e^{-\frac{tKd}{V}} \quad (6)$$

Where C_0 was the initial Urea concentration in blood, C_e is the final Urea concentration in blood, both in mmol/L, was used with input parameters such as blood, the dialysate flow rate in mL/min, initial concentration of Urea in a blood sample and the final desired concentration of Urea in the blood and then Eq. (5) calculates the clearance of the dialyzer. Further input parameters include the patient's weight based on gender. Based on the patient's dry weight and gender, the value of Urea distribution volume is calculated using equations for males' and females' volume distributions.

$$V_{male} = 0.58DW \quad (7)$$

$$V_{female} = 0.55DW \quad (8)$$

Where DW is the patient's dry weight in kilograms, the equation below incorporates all the above-calculated parameters and plots change in concentration over time in minutes. Table 5 contains values of parameters that were kept constant and utilized in this model.

Table 5 Values of parameters used for Urea concentration vs. Time model

Parameter	Value	Units
Dialysate flow rate, Qd	500	mL/min
Initial Urea concentration in a blood sample, C_i	30	mmol/L
Final Urea concentration in a blood sample, C_e	13	mmol/L
Patient's weight, DW	70	Kg

3.2.3 Effect of flow orientation on Urea clearance

The effect of flow direction is always substantial in case fluids come into contact with one another, whether directly or through a semipermeable barrier. For example, in clinical arrangements, blood and dialysate contact counter-currently across a hollow fiber module. The rationale behind this flow arrangement is that counter-current flow assists in maintaining a constant concentration gradient because fresh dialysate keeps coming in

contact with blood containing sufficient solutes [60]. However, how much is the quantitative effect of this difference of directions upon the clearance of Urea was explored in this study. For counter-current flow, the clearance of Urea was evaluated using Eq. (5), while for co-current flow, clearance was calculated using the Eq. (9).

$$D = Qb \frac{1 - e^{-\left(\frac{KA(1 + \frac{Qb}{Qd})}{Qb}\right)}}{1 + \frac{Qb}{Qd}} \quad (9)$$

The model required blood flow rate, the concentration of Urea in blood, and dialysate sample as inputs. The overall mass transfer area coefficient is calculated through concentration values, which are further used in both co and counter-current clearance equations.

Table 6 Values of parameters used for finding Urea clearance in Co and Counter current flow arrangement

Parameter	Value	Units
Blood flow rate, Qb	250	mL/min
Overall mass transfer coefficient, K _o A	1000	mL/min
Concentration of Urea in a blood sample, C _e	30.3	mmol/L
Concentration of Urea in dialysate sample, C _d	9.8	mmol/L

3.2.4 Effect of overall mass transfer area coefficient on Urea clearance with a varying dialysate flow rate

The overall mass transfer coefficient values are always mentioned in the specification manual of each commercially available hemodialyzer. The manufacturer calculates these values of overall mass transfer coefficients under certain blood and dialysate flow rates. Here, K_oA was initially considered constant for a certain dialyzer, but investigation showed that varying dialysate flow rates result in varying values [61]. As varying dialysate flow rates vary the values of K_oA, the changes in values of K_oA produce a

change in the value of clearance. For finding the effect of changing K_oA values on clearance, Eq. (5) was used with different values of K_oA . Dialyzers with K_oA up to 600 mL/min represent moderate efficiency, while those above 600 mL/min are considered high-efficiency dialyzers [17]. Other than the input values of K_oA , the value for blood flow rate was provided.

Table 7 Values of parameters used for evaluating the effect of overall mass transfer area coefficient on Urea clearance

Parameter	Value	Units
Blood flow rate, Q_b	250	mL/min
Mass transfer area coefficient (Low efficiency)	500	mL/min
Mass transfer area coefficient (High efficiency)	800	mL/min

3.2.5 Changes in Urea clearance with change in hollow fiber dimensions

For investigating the effect of change in hollow fiber dimensions on Urea clearance, Eq. (10) was used to find the area of hollow fibers:

$$A_{fiber} = (2\pi)(r)(l) \quad (10)$$

The value of one of the parameters between length and radius was kept constant. From the value of a single fiber, Eq. (11) was used to find out the total area of the membrane:

$$A_{dialyzer} = (A_{fiber})(N_o) \quad (11)$$

The membrane area was used in Eq. (5) to determine the change in Urea clearance over a certain range of changes in specific fiber dimensions. The user will enter the initial and final values of these dimensions to evaluate the clearance value over a specific fiber length or radius range. Also, as the program aims to compare the effect of change in fiber dimensions, blood and dialysate flow rates are kept constant.

Table 8 Values of parameters for evaluating change in Urea clearance with change in hollow fiber dimensions

Parameter	Value	Units
Blood flow rate, Qb	300	mL/min
Dialysate flow rate, Qd	500	mL/min
Hollow fiber initial length, Li	20	Cm
Hollow fiber final length, Lf	60	Cm
Hollow fiber initial radius, Ri	100	μm
Hollow fiber final radius, Rf	220	μm

3.2.6 Effect of residual renal clearance on standard and equilibrated hemodialysis adequacy

There have been multiple attempts to find the most accurate dialysis dose equation. The significant difference lies in the variables required to calculate adequacy using a particular equation. The most commonly used equations are of a single pool, equilibrated, and standard KT/V. Here we have analyzed standard KT/V and equilibrated KT/V as both of these equations incorporate residual renal function, which plays a vital role in assessing morbidity and mortality of ESRD patients. A study reported that patients with healthy and preserved residual renal function had a lower mortality rate than patients with no or minimal residual renal clearance [62]. Therefore, Eq. (12) was used to calculate eKT/V with varying residual renal function:

$$\frac{eKt}{V} = 4.5 \times \frac{Kru}{V} \quad (12)$$

$$\frac{stdKT}{V} = \frac{10,080 \frac{1-e^{-eKt/V}}{t}}{\frac{1-e^{-eKt/V}}{eKt/V} + \frac{10,080}{Ft} - 1} \quad (13)$$

Also, the change in values of stdKT/V with varying numbers of sessions per week was evaluated and analyzed.

Table 9 Values of parameters for evaluating the effect of residual clearance on standard and equilibrated hemodialysis adequacy

Parameter	Value	Units
Time for a dialysis session, t	120	Min
Number of sessions per week, F	3,4,5	-
Patient's post-dialysis weight	70	Kg

3.3 Simulation Scenarios

Different simulation scenarios were utilized in models considering the real-time limitations and ranges of various parameters. The purpose behind these simulation scenarios was to better understand the optimization of parameters.

3.3.1 Simulation scenario for change in Urea clearance rate with varying blood and dialysate flow rate

From Table 3, initially, the value of the dialysate flow rate is kept fixed at 500 mL/min while the value for the blood flow rate is kept at 300 mL/min and then raised to 400 mL/min. The value of dialysate in most cases is two times the value of the blood flow rate, whereas in most cases, it is kept between 500 mL/min to 800 mL/min [63].

Similarly, for the Urea clearance versus dialysis flow rate model, the overall mass transfer coefficient is equal to 1000 mL/min, the blood flow rate is kept constant at 400 mL/min while the dialysate flow rate is varied from 200 to 1000 mL/min.

3.3.2 Simulation scenario for change in Urea concentration with time

The model to find the change in Urea clearance for change had a dialysate flow rate value equal to 500 mL/min while values for initial and final blood sample concentration present in Table 5 were taken from the literature [64]. The patient's weight is assumed to be 70 Kg, as is the nominal weight of an adult human being. Figure 14 shows the app's user interface to determine the drop in Urea concentration with time.

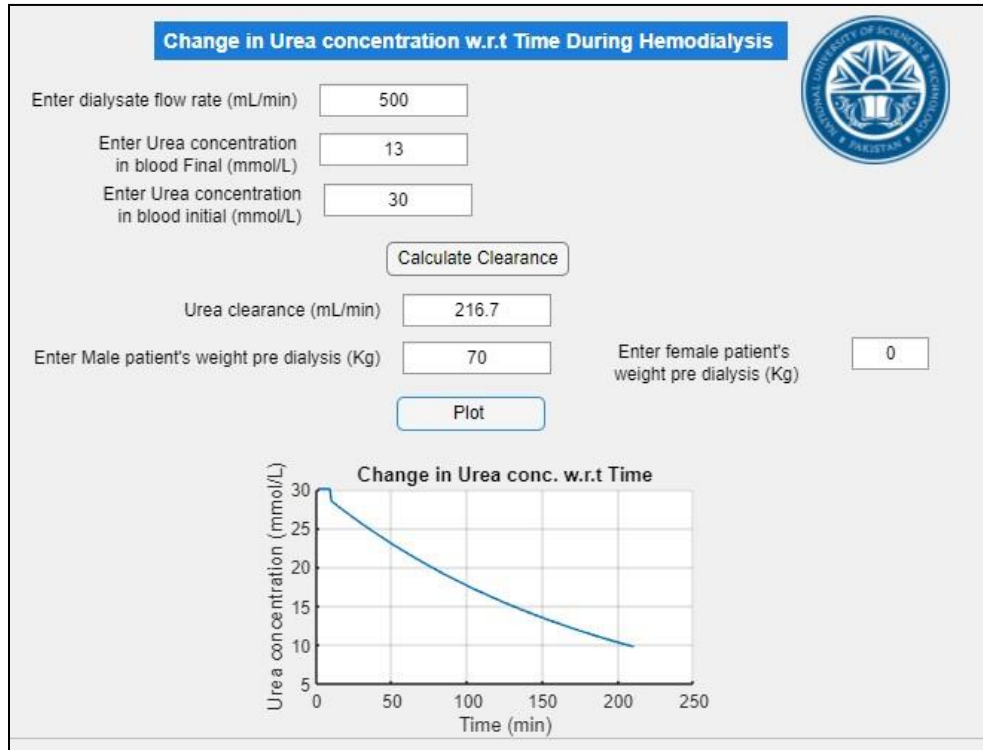


Figure 14 User interface of the app to find change in Urea concentration with change in time

3.3.4 Simulation scenario for the effect of flow orientation on clearance

Table 6 shows the input values provided to the model for predicting flow orientation's effect on Urea clearance. The overall mass transfer coefficient is again supposed to be 1000 mL/min as it is the value for a high-efficiency dialyzer. The values for the concentration of toxins are taken from the literature [64]. Figure 15 compares the flow orientations of both fluids within a dialyzer.

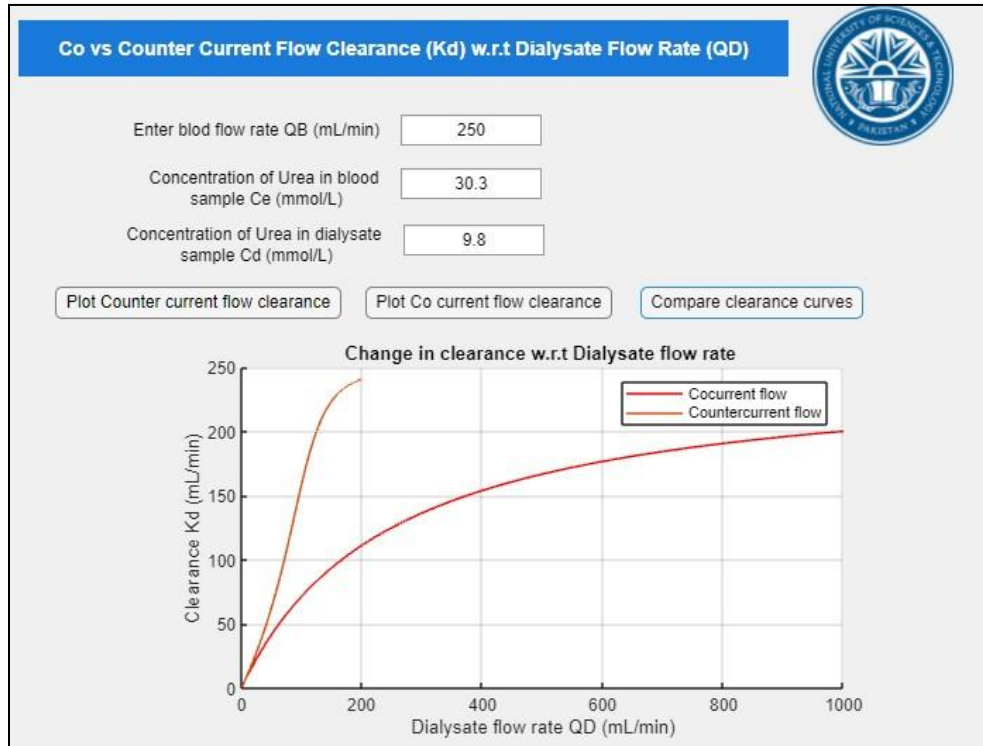


Figure 15 User interface of the app to calculate the change in clearance with a change in flow orientation

3.3.5 Simulation scenario for the effect of overall mass transfer coefficient

The bifurcation between a high and low-efficiency dialyzer done by most authors based on the mass transfer area coefficient shows that dialyzers having K_oA less than 750 mL/min are low efficiency. In contrast, those above 750 mL/min are classified as high-efficiency dialyzers. For this reason, a value of K_oA was taken for a low and a high-efficiency dialyzer. Figure 16 shows the effect of change in K_oA values while keeping all other parameters constant.

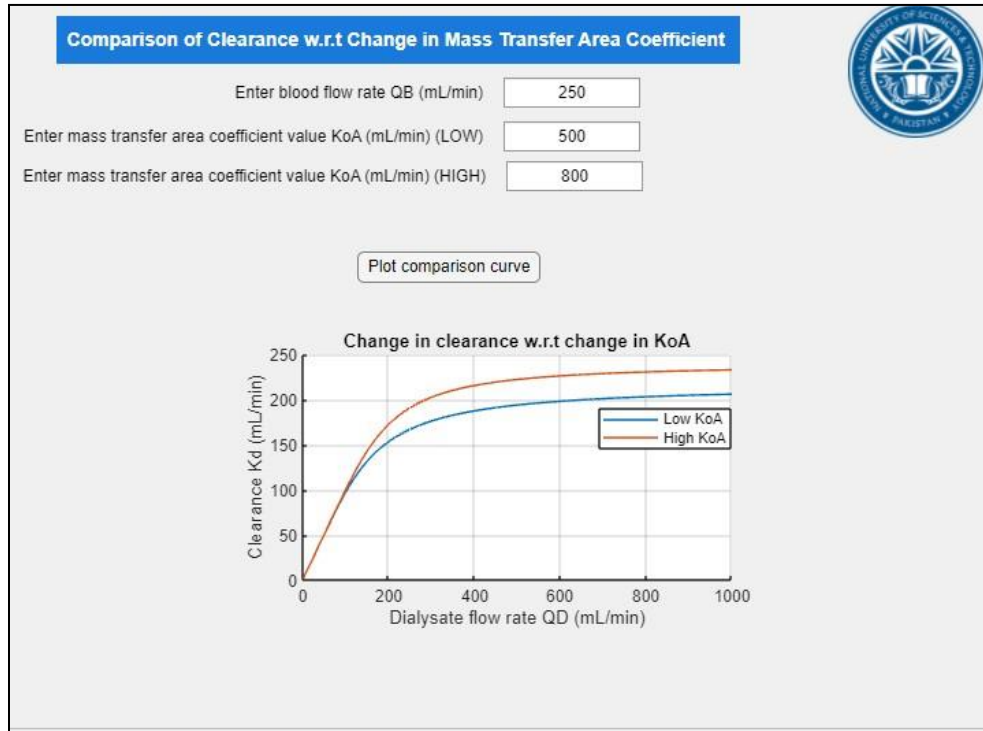


Figure 16 User interface of the app to calculate the change in Urea clearance with change in overall mass transfer coefficient

3.3.6 Simulation scenario for the effect of hollow fiber dimension on clearance

The length of a hollow fiber used for hemodialysis varies in the range of 20-4 cm, while hollow fibers' diameter varies between 180-220 μm [65]. The values of blood and dialysate flow rate were kept fixed to find the change in clearance only due to changing dimensions of hollow fibers. Figure 17 shows the app's user interface used to evaluate the effect on clearance with changing dimensions of hollow fibers.

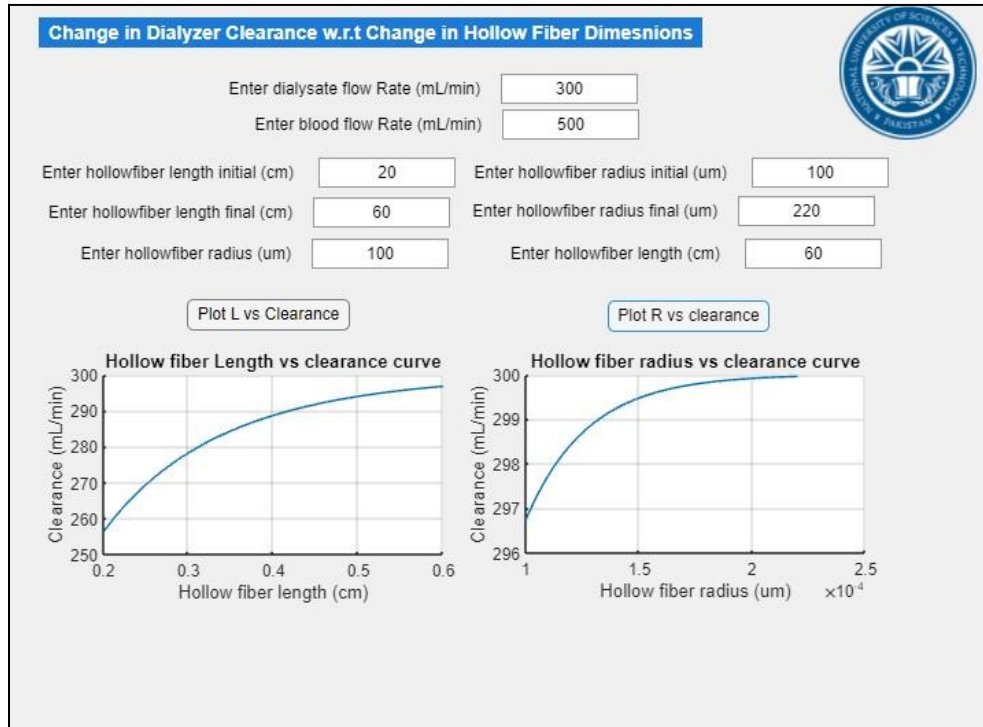


Figure 17 User interface of the app to calculate the change in Urea clearance with a change in dimensions of the hollow fibers

3.4 Performance Metrics

3.4.1 Mean Squared Error

Mean squared error is usually utilized to find the quality of a prediction or an estimation model. The formula for mean squared error measures the difference between the model's predicted and available values. The equation to find the mean squared error is

$$\text{Mean square error (MSE)} = \frac{1}{n} \sum_{i=1}^n (Y_i - \hat{Y}_i)^2 \quad (14)$$

In Eq. (14), Y_i is the observed value, and \hat{Y}_i is the predicted value of the model, and n is the number of values in the data set.

3.4.2 Coefficient of determination

R squared, or the coefficient of determination represents the difference between the predicted and actual values. Its value varies between 0 and 1. 0 denotes that the model cannot explain any of the values in the data

set. In contrast, values closer to 1 depict that model can be used to describe the variation occurring in the values across various input values. The equation to find R^2 is

$$R^2 = \frac{\sum_{i=1}^n (Y_i^F - \bar{Y})^2}{\sum_{i=1}^n (Y_i - \bar{Y})^2} \quad (15)$$

In Eq. (15), Y_i^F represents the model-predicted values, \bar{Y} Represents the mean of actual values, Y_i represents the actual values and n is the number of values in the dataset.

Chapter 4

Results and Discussion

4.1 Membrane Module Design Results

The models were developed to analyze the effect of varying parameters on the Urea clearance and compare the current model results with the existing literature.

4.1.1 Change in Urea clearance rate with blood and dialysate flow rate

The model was developed to find the change in the clearance values of Urea and the change in blood and dialysate flow rates while keeping all the other parameters at a constant value. Initially, the value of the dialysate flow rate was kept constant at 500 mL/min while the blood flow rate value varied from 300 mL/min to 400 mL/min. Figure 18 shows that the models of Islam and Tooba are in close agreement with each other, while the current model is in relatively good agreement with the experimental data.

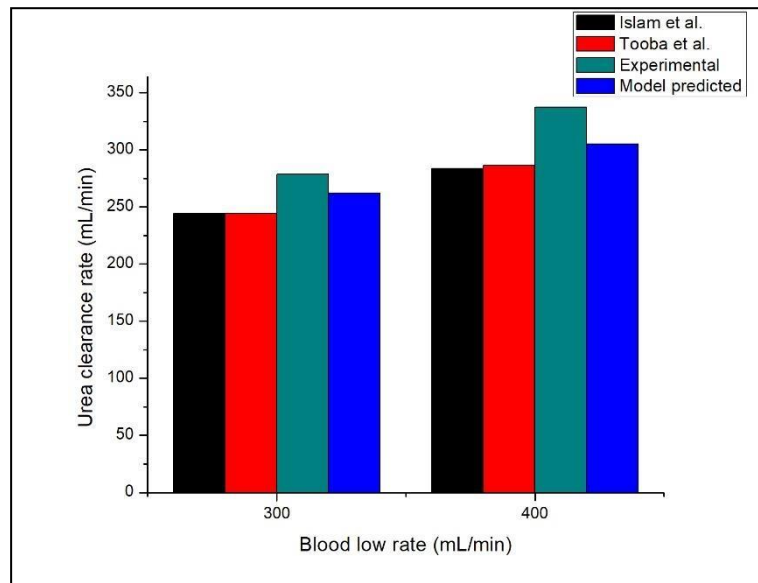


Figure 18 Urea clearance values for in-vitro and in-silico scenarios with varying blood flow rate and constant dialysate flow rate ($Q_d=500$ mL/min)

Table 10 Comparison of model results with the literature [55, 58, 66]

Blood flow rate (mL/min)	Model predicted	Tooba et al.	Islam et al.	Experimental data (Polyflux 210H)	Percentage difference between Model-predicted and Manufacturer data	Percentage difference between Tooba et al. and Manufacturer data
300	262	247.77	244.62	281	6.76	11.82
400	305	289.52	286.40	339	10.03	14.59

Table 10 shows that the percentage difference between the models' predicted clearance and experimentally found clearance is due to the absence of ultrafiltration flux across the membrane, which is not accommodated in the current model. Also, the difference between model values of clearance and clearance values of Islam and Tooba is because parameters such as tortuosity and porosity are not accommodated. This model overestimates the clearance values. Also, since the Polyflux 210H is a high-efficiency hemodialysis membrane ($K_oA = 1452$ for Urea), the K_oA value was considered 1000 mL/min to compare the model with it. However, assuming the overall mass transfer coefficient values closer to 1452 mL/min brings the model more aligned with experimental data.

The model was further extended to evaluate the change in the Urea clearance with varying dialysate flow rate at constant blood flow rate value.

The model-predicted clearance curves were plotted with Islam et al. and Tooba et al. in silico model results [55, 66]. The comparison shows an increase in clearance as the dialysate flow rate increases. Initially, the model predicted values are much lower than previous in silico models. This difference decreases until around the dialysate flow rate of 400 mL/min. The predicted clearance becomes greater than in previous in silico models. The underlying reason behind this steep increase is mainly due to the non-inclusion of tortuosity and porosity parameters of the membrane. The increasing trend

continues as per Eq. (5). However, further investigations revealed that if the value of the dialysate flow rate is further increased, the curve becomes a plateau.

Any further increase in the value of the dialysate flow rate does not result in any increase in clearance values. Also, if the blood flow rate value is not kept constant at 400 mL/min, the clearance values would further enhance. However, blood and dialysate flow rate values are kept between specific ranges in clinical practices. For example, the average variation range is from 250 mL/min to 300 mL/min depending on the patient profile and quality of vascular access. A study showed that an increase of 30% in the value of blood flow rate results in around a 23% increase in Urea clearance, provided that all other parameters are kept constant [67]. However, lower blood flow rates can also lead to reduced adequacy, which promotes atherosclerosis, infection, and mortality [68]. In addition, increasing value beyond this range can cause complications related to cardiovascular function in the human body.

Similarly, in clinical arrangements, the dialysate flow values are kept between 500 mL/min to 800 mL/min. Higher dialysate flow rates increase adequacy and clearance. However, it also increases the amount of dialysate utilized in a dialysis session, increasing the overall cost of a dialysis session. A study showed that increasing the dialysate flow rate from 500 mL/min to 800 mL/min increased the Urea K_oA by an average of $14 \pm 7\%$ as it decreases the thickness of a thick fluid layer on the dialysate side. It is also suggested that it is due to improved flow distribution of dialysate [69]. Modeling the Urea clearance equation also shows a plateau of the clearance curve after a particular increase in the value of the dialysate flow rate.

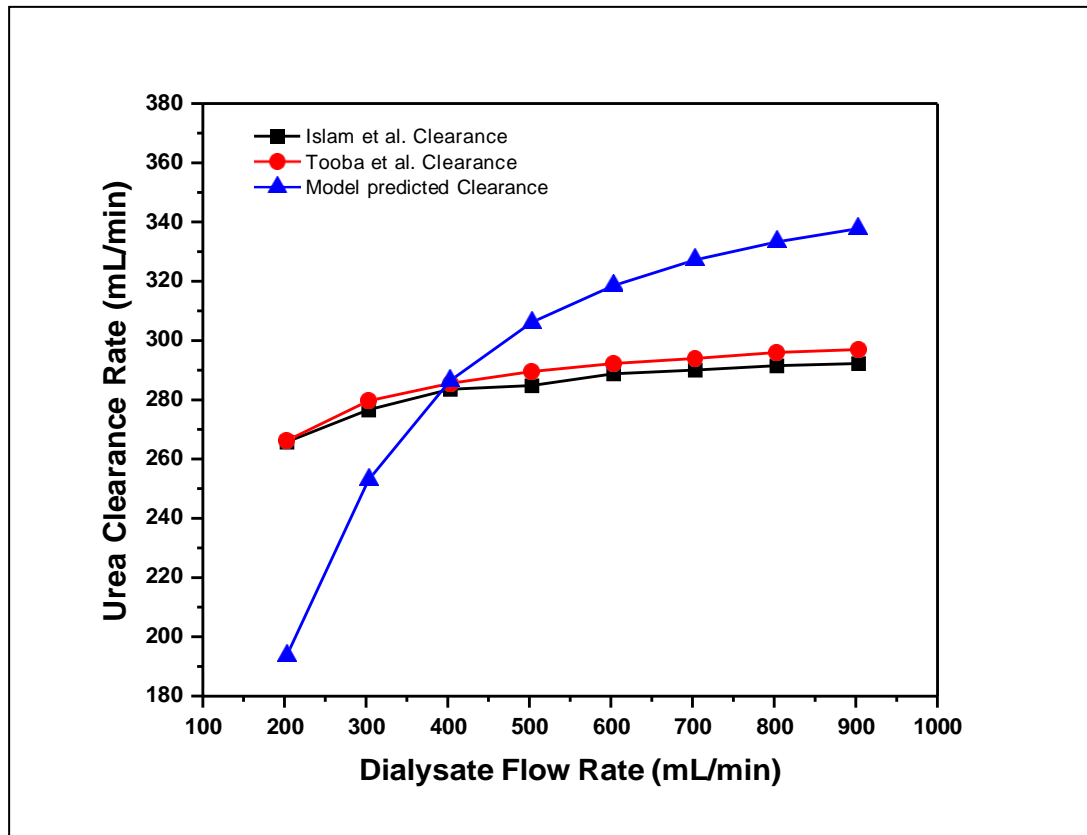


Figure 19 Model predicted Urea clearance vs. in silico solute clearances plotted at increasing dialysate flow rate at $Q_b=400$ mL/min

Table 11 Percentage difference between this model and previous models [55, 66]

Dialysate flow rate (mL/min)	Tooba et al. clearance (mL/min)	Islam et al. clearance (mL/min)	Model predicted clearance (mL/min)	Percentage difference b/w Model and Tooba et al.	Percentage difference b/w Model and Islam et al.
203	266.23	265.73	193.75	-37.41%	-37.15%
303	279.61	276.64	252.97	-10.53%	-9.35%
403	285.56	283.58	286.47	0.32%	1.01%
503	289.52	284.81	306.21	5.45%	6.99%

603	292.25	288.78	318.60	8.27%	9.36%
703	293.98	290.02	327.20	10.15%	11.36%
803	295.96	291.50	333.30	11.20%	12.54%
903	296.96	292.25	337.80	12.09%	13.48%

4.1.2 Variation in Urea concentration with time during hemodialysis

The plotted change in the concentration of Urea over time showed that a single pool model predicts an exponential decrease in the toxin concentration over time. A single pool model considers the whole patient's body into a single compartment and the extracorporeal circuit or dialyzer into a separate pool. To find the time required to reduce toxin concentration to a certain level, the single pool model first calculates a dialyzer's clearance value. Here it must be noted that an advantage of using this model is that it allows the calculation of dialyzer clearance before the single pool equation is solved. Based on the blood, dialysate flow rates, and initial and final concentrations of the toxin in the patient's blood, it calculates clearance which in the given scenario was calculated to be 216 mL/min. Also, the model calculates the toxin distribution volume, which for a 70 kg male patient in our case, was calculated to be 4.09×10^4 mL. In the case of a female patient, Eq. (7) and Eq. (8) are utilized to find the distribution volume of the toxin. The final equation (6) incorporates the dialyzer clearance and the toxin distribution volume to find the Urea concentration at a specific time.

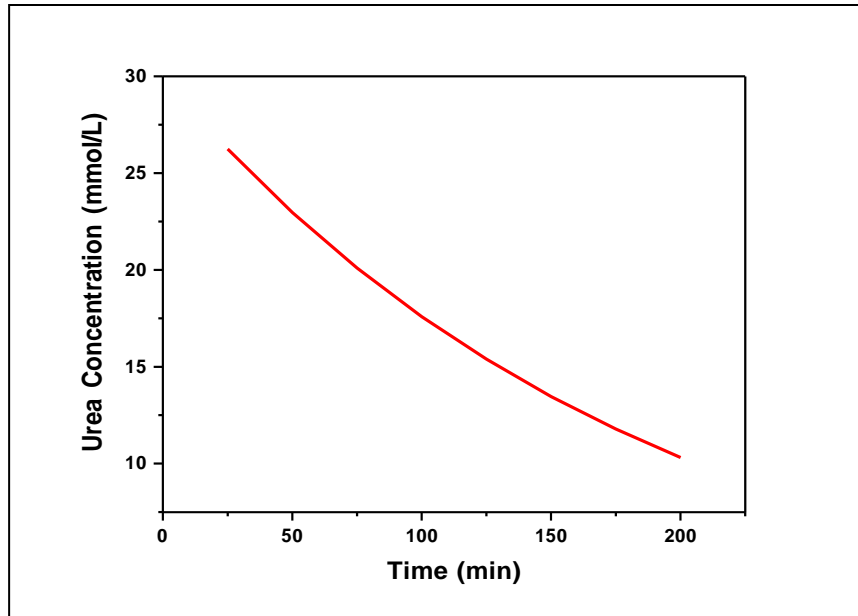


Figure 20 Graph showing the decrease in Urea concentration over time

Table 12 Change in Urea concentration with time

Time (min)	Urea concentration (mmol/L)
25	26.25
50	22.97
75	20.10
100	17.59
125	15.40
150	13.47
175	11.79
200	10.32

4.1.3 Effect of flow orientation on Urea clearance

The change in urea clearance rate for both orientations is negligible initially as the dialysate flow rate increases. However, as the dialysate flow rate approaches a value of 100 mL/min, the difference in clearance starts becoming prominent. The underlying reason behind the similar clearances for both flow orientations initially is the negligible convective mass transfer when the dialysate flow rate is less. However, as the value for the dialysate flow rate increases, the convective transport starts adding to the diffusive mass transfer. It becomes the dominant mass transfer phenomenon at a higher dialysate flow rate when the fresh dialysate is constantly exposed to blood.

On the other hand, as dialysate flow rates are increased for co-current flow, the concentration gradient approaches a constant value, after which it does not alter further, and clearance becomes constant since the concentration gradient is the primary driving force in hemodialysis. The counter-current arrangement is utilized in clinical practices since it exposes fresh dialysate to blood to maintain a high concentration gradient [60]. Table 13 also shows that as dialysate flow approaches 500 mL/min value, the percentage difference between clearance starts changing with a constant rate since at higher dialysate flow rates, the maximum concentration gradient is approached, and clearance varies very to a minimal extent with further increasing dialysate flow rate. Further extending these curves gives plateaus for both flow arrangements as the effect of the dialysate flow rate becomes constant.

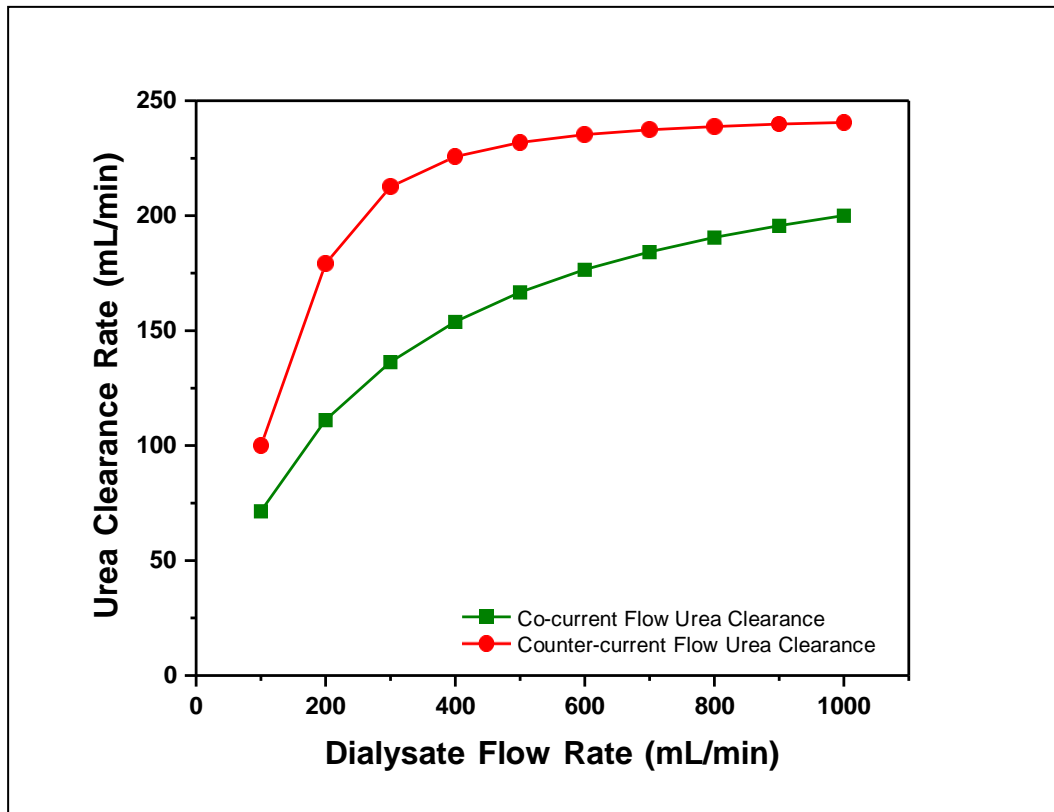


Figure 21 Difference in Urea clearance with change in flow orientation at different dialysate flow rates

Table 13 Percentage difference in clearance rate with increasing dialysate flow rates for Co and Counter current flow arrangements

Dialysate flow rate (mL/min)	Co-current flow Urea clearance (mL/min)	Counter current flow Urea clearance (mL/min)	Percentage difference between co and counter-current clearance
100	71.43	99.85	28.46%
200	111.11	179.15	37.98%
300	136.36	212.61	35.86%
400	153.85	225.69	31.83%
500	166.67	231.86	28.12%
600	176.47	235.26	24.99%

700	184.21	237.37	22.40%
800	190.48	238.79	20.23%
900	195.65	239.80	18.41%
1000	200.00	240.55	16.86%

4.1.4 Effect of varying overall mass transfer area coefficient on Urea clearance

The effect of changing values of the overall mass transfer coefficient (K_oA) on clearance is negligible until at a dialysate flow rate of 100 mL/min, where it becomes prominent. This effect on clearance keeps on becoming prominent until around 30 mL/min, after which both the curves start forming plateaus, and the percentage difference between both clearance rates becomes stable. Further, increasing the dialysate flow rate produces no change in the clearance of Urea for both cases. For both scenarios, the concentration gradient reaches a maximum value, and any further increase in dialysate flow rate causes no assistance in incrementing the concentration gradient. Also, for initial similar clearance patterns, the rationale is that at low dialysate flow rates, diffusion is the dominant mass transport phenomena, and diffusion rate is dependent on the dialysate flow rate to a considerable extent at lower dialysate flow rates. The increase in Urea clearances for both values of K_oA is because fluid mixing is good at higher dialysate flow rates and reduces the film resistance for smaller molecules [70]. The solute clearing efficiency of a dialyzer is quantified by K_oA which is the overall mass transfer coefficient and is often referred to as the efficiency of the dialyzer [17]. The manufacturers mention the values for K_oA under specific blood and dialysate flows. Initially, the value of K_oA was supposed to be constant for a certain dialyzer; however, investigations have refuted this supposition as with increasing dialysate flow rates, flow distribution within the fiber bundle enhances, thus enhancing the overall mass transfer coefficient [71]. Classification of dialyzers is also often done based on this parameter, with low-efficiency dialyzers having K_oA less than 500 mL/min, moderate-efficiency dialyzers having 500 to 600 mL/min, and high-efficiency dialyzers having K_oA greater than 600 [17]. Several researchers have theoretically predicted the effects of increasing dialysate flow rates on the K_oA .

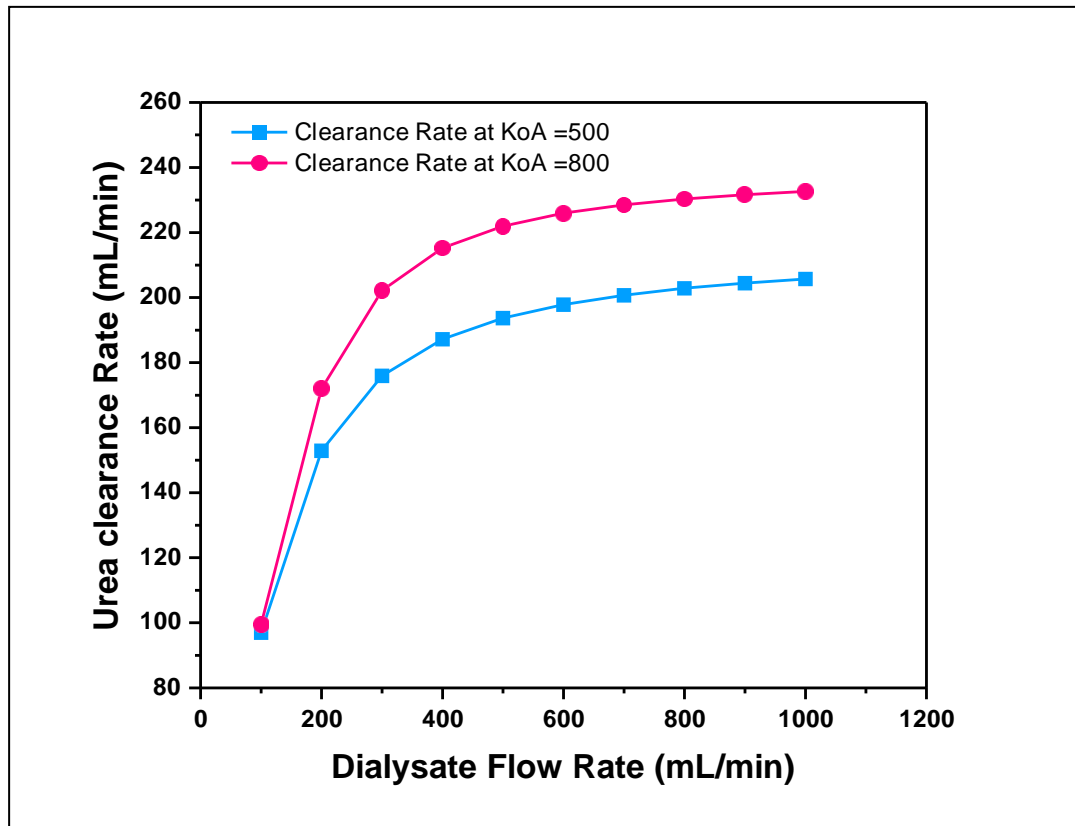


Figure 22 Effect of overall mass transfer area coefficient on clearance with changing dialysate flow rates

Table 14 Percentage difference in clearance of dialyzers with low and high overall mass transfer area coefficient

Dialysate flow rate (mL/min)	Clearance rate at $K_oA =500$ (mL/min)	Clearance rate at $K_oA =800$ (mL/min)	Percentage difference in clearance with low and high K_oA
100	96.95	99.50	2.57%
200	152.87	171.94	11.09%
300	175.90	202.18	13.00%
400	187.16	215.21	13.03%
500	193.65	221.93	12.74%
600	197.82	225.90	12.43%
700	200.70	228.48	12.16%

800	202.81	230.27	11.92%
900	204.42	231.59	11.73%
1000	205.69	232.60	11.57%

4.1.5 Changes in Urea clearance with change in hollow fiber dimensions

As the length of dialyzer fiber increases, there is an increase in the value of the Urea clearance rate. The clearance rate, however, is more for the current model than the previous ones. This difference is because the current model incorporates radius, fiber length, dialyzer's K_oA , and blood and dialysate flow rates. In contrast, previous models include tortuosity, the porosity of layers, and the sizes of pores of each fiber, due to which the value of Urea clearance is underestimated compared to the current model. The percentage difference is relatively less with Tooba et al. than with Islam et al., as the former model was based on the tortuous pore diffusion model. Also, the model shows that further increasing the fiber length produces a plateau for Urea clearance without any significant increase in Urea clearance. Increasing the length also adds to the dialyzer cost, ultimately increasing the cost of the process for patients.

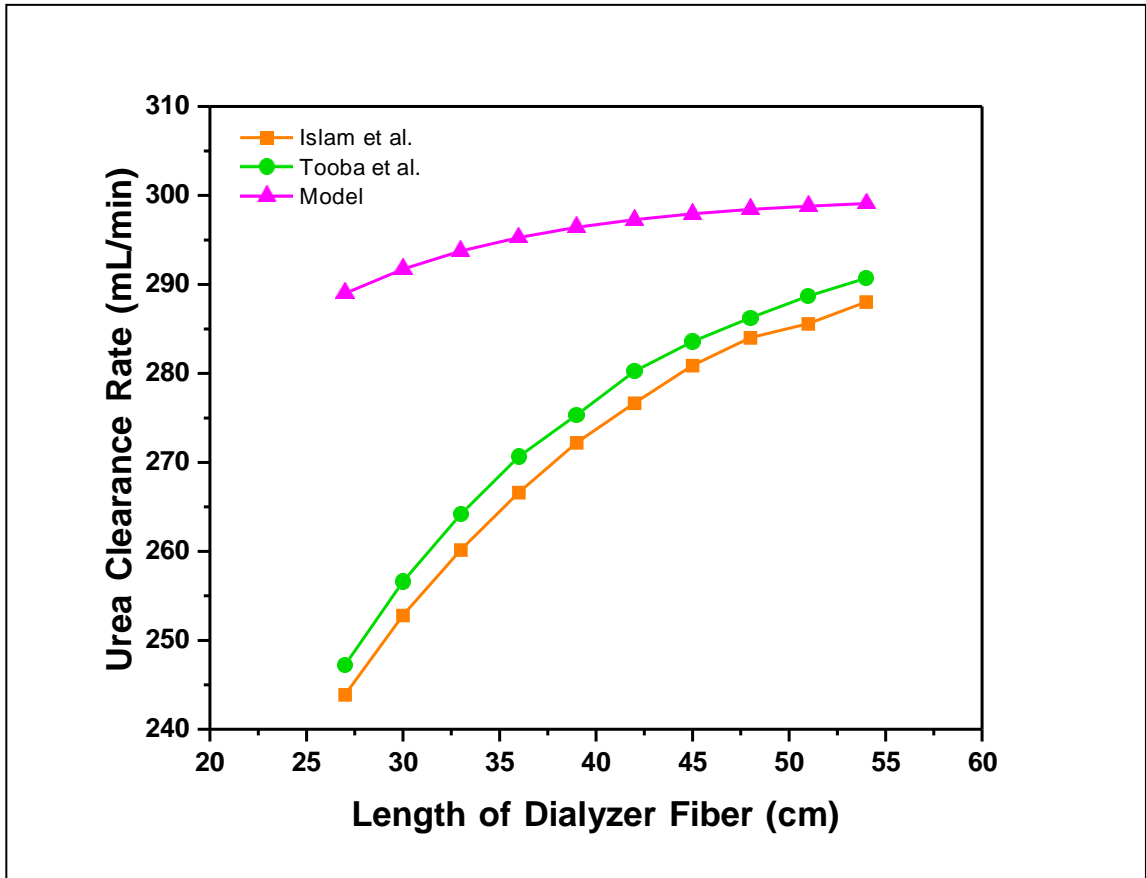


Figure 23 Change in Urea clearance rate with change in length of hollow dialyzer fiber

Table 15 Percentage difference between models showing a change in Urea clearance with a change in length of fiber

Length of dialyzer fiber (cm)	Islam et al. Urea clearance rate (mL/min)	Tooba et al. Urea clearance rate (mL/min)	Model Predicted Urea clearance rate(mL/min)	Percentage difference b/w model and Islam et al.	Percentage difference b/w model and Tooba et al.
27	243.89	247.23	289.00	15.61%	14.45%
30	252.80	256.59	291.72	13.34%	12.04%
33	260.16	264.17	293.75	11.44%	10.07%
36	266.62	270.64	295.27	9.70%	8.34%
39	272.20	275.32	296.42	8.17%	7.12%
42	276.66	280.22	297.28	6.94%	5.74%

45	280.89	283.57	297.93	5.72%	4.82%
48	284.01	286.24	298.43	4.83%	4.08%
51	285.57	288.69	298.80	4.43%	3.38%
54	288.03	290.70	299.09	3.70%	2.80%

As was the case for the length of hollow fibers versus clearance, the same is valid with the radius of hollow fibers, which is the increase in radius results in an increase in Urea clearance. The percentage difference between the model and previous models is somewhat similar to the percentage difference obtained for the hollow fiber length versus the Urea clearance model. Also, the percentage difference between the current models with Tooba et al. is less compared to Islam et al., as the former model was based on the tortuous pore diffusion model, which considers the factors that cause hindrance within the porous medium. The model further shows that increasing the fiber radius produces a plateau for Urea clearance without any significant increase in Urea clearance. Increasing the radius also adds to the dialyzer cost, ultimately increasing the cost of the process for patients.

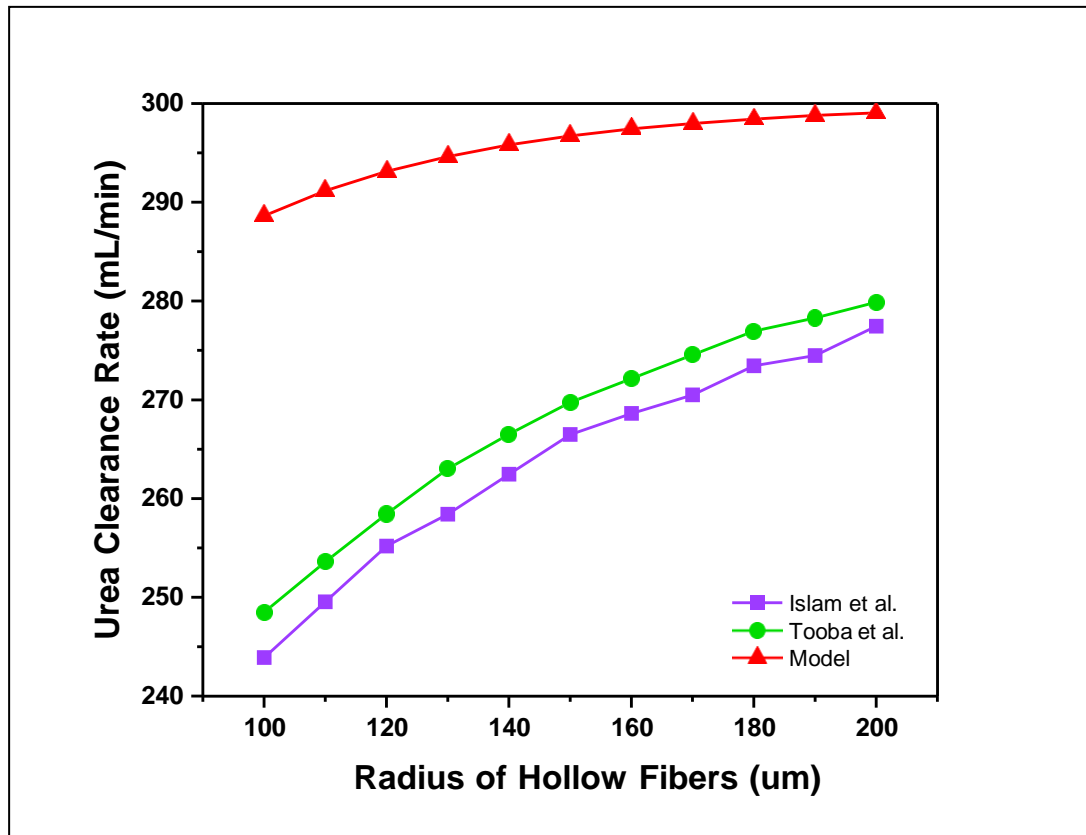


Figure 24 Change in Urea clearance rate with change in radius of hollow fiber

Table 16 Percentage difference between models showing a change in Urea clearance with a change in the radius of a fiber

The radius of hollow fibers (um)	Islam et al. Urea clearance rate (mL/min)	Tooba et al. Urea clearance rate (mL/min)	Model Predicted Urea clearance rate(mL/min)	Percentage difference b/w model and Islam et al.	Percentage difference b/w model and Tooba et al.
100	243.90	248.49	288.64	15.50%	13.91%
110	249.55	253.60	291.18	14.30%	12.91%
120	255.20	258.45	293.14	12.94%	11.83%
130	258.42	263.02	294.65	12.29%	10.74%
140	262.46	266.51	295.82	11.28%	9.91%
150	266.49	269.73	296.73	10.19%	9.10%
160	268.63	272.14	297.44	9.69%	8.51%

170	270.50	274.55	297.99	9.23%	7.87%
180	273.45	276.96	298.43	8.37%	7.19%
190	274.50	278.29	298.80	8.13%	6.86%
200	277.46	279.89	299.06	7.22%	6.41%

4.1.6 Change in values of standard and equilibrated hemodialysis adequacy with increasing residual renal clearance

With the increasing number of sessions per week and the improvement of residual renal function, the values of std KT/V also improve, as shown in Figure 25. This improvement in std KT/V becomes more prominent with improvement in residual renal clearance. Also, with an increasing number of dialysis sessions per week, with some residual renal clearance, it can be seen that the increase in std KT/V is two times the initial value, as shown in Table 17. It validates that improved residual renal clearance plays a vital role in dialysis patients. A study showed that patients on hemodialysis therapy that had preserved residual renal function one year after dialysis initiation had a 30% lower mortality risk and a 31% lesser risk of cardiovascular death [72]. This relation between residual renal function and mortality indicates that residual clearance plays a vital role in the excretion of uremic toxins [73]. Patients suffering from ESRD have a minimal value of residual renal clearance if they have any at all. However, dialysis is usually recommended for patients with residual clearance of less than 15 mL/min [17]. For patients having minimal residual clearance, an acceptable value of std KT/V can be achieved by increasing the number of sessions per week.

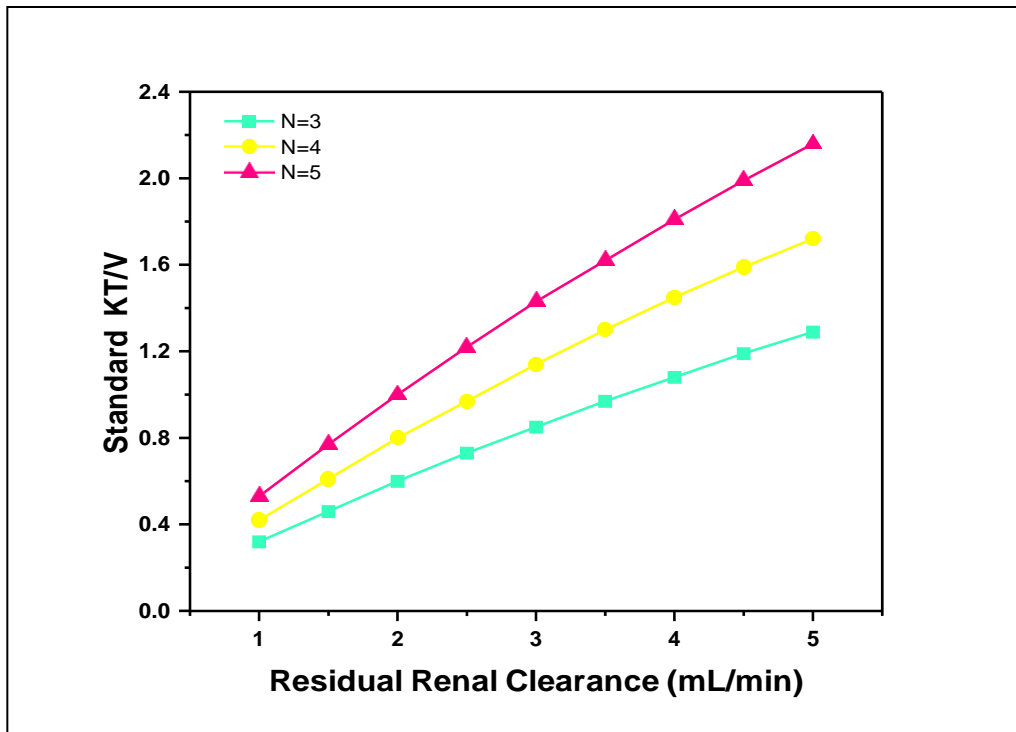


Figure 25 Change in std KT/V with increasing residual renal function at different numbers of hemodialysis sessions per week

Table 17 Increase in std KT/V with an increase in the number of hemodialysis sessions per week

Residual renal clearance (mL/min)	std KT/V at N=3	std KT/V at N=4	std KT/V at N=5	Change in std KT/V when N=3-->4	Change in std KT/V when N=4-->5
1	0.32	0.42	0.53	0.1	0.21
1.5	0.46	0.61	0.77	0.15	0.31
2	0.6	0.8	1	0.2	0.4
2.5	0.73	0.97	1.22	0.24	0.49
3	0.85	1.14	1.43	0.29	0.58
3.5	0.97	1.3	1.62	0.33	0.65
4	1.08	1.45	1.81	0.37	0.73
4.5	1.19	1.59	1.99	0.4	0.8
5	1.29	1.72	2.16	0.43	0.87

4.2 Discussion of Results

4.2.1 Validation of the models

The mathematical models were developed using MATLAB 2022 with a specific fixed value for certain inlets while simultaneously varying the values of other parameters. The models were validated by comparing them with Islam et al. and Tooba et al., while in some cases, a comparison with experimental work was also made [55, 66]. In Figure 18, the values of dialysate flow rate are kept constant at 500 mL/min while the value of blood flow rate has two different values of 300 mL/min and 400 mL/min. The model-obtained results are plotted along with previous studies and with experimental data available. The experimental values of clearance present in the literature contain a combined effect of ultrafiltration and diffusion occurring during hemodialysis. The percentage difference between the model predicted by the Tooba et al. and experimental values is because of ultrafiltration occurring across the membrane, which was not included in the previous or current works. However, the values predicted by the previous model of Tooba et al. for diffusive transport across the membrane agree well with Islam et al. results.

In this model, a model that compares the change in the value of Urea clearance with changing dialysate flow rate was compared for validation with Islam et al. and Tooba et al. work. The blood flow rate value was kept constant at 400 mL/min while the value of the dialysate flow rate varied from 200 mL/min to 1000 mL/min. The value of all other parameters was kept constant. Figure 19 shows that for all three models, increasing the dialysate flow rate increases the value of clearance; however, the change between clearance values of the current model is more than that compared to previous models due to both the previous models included parameters such as porosity and tortuosity of the membrane.

Figures 23 and 24 exhibit the change occurring in the clearance rate of Urea with a change in the dimensions of the hollow fibers. As the length of hollow fibers is varied from 25-55 cm, there is an increase in the Urea clearance. However, the increase for the current model is more than the increase compared to the previous models, as the previous works include factors like tortuosity and porosity. Due to their effect, the value of Urea clearance is underestimated, as shown in Figure 23. Table 15 shows the percentage difference

between the clearance rates for the compared models. The percentage difference between the current model and the model by Tooba et al. is less compared to the difference between this model and Islam et al.

Figure 24 shows the change in clearance rate with a change in the radius of hollow fibers. Similar to the change in clearance for length, the change in clearance for radius also shows an increasing trend with an increase in the radius value. Table 16 shows the percentage difference between the clearance rates for the compared models. The percentage difference between the current model and the model by Tooba et al. is less compared to the difference between this model and Islam et al.

4.2.2 Mean Square Analysis

The mean squared error value is usually utilized to find the quality of a prediction or estimation model. The formula for mean squared error measures the difference between the model-predicted and the available values. Eq. (14) is used to find the mean squared error. In which, Y_i is the observed value, and \hat{Y}_i is the predicted value of the model, and n is the number of values in the data set.

Table 18 shows the calculations for finding out the Mean squared error for a model that calculates the clearance values with changing dialysate flow rates.

Table 18 Table showing Mean square error for model calculating clearance w.r.t dialysate flow rate

Dialysate flow rate (mL/min)	Tooba et al. clearance (mL/min)	Islam et al. clearance (mL/min)	Model predicted clearance (mL/min)	Difference bw model and Tooba et al. clearance (Yi-Yi [^])	Difference bw model and Tooba et al. clearance squared	Difference bw model and Islam et al. clearance (Yi-Yi [^])	Difference bw model and Islam et al. clearance squared
203	266.23	265.73	193.75	72.48	5253.35	71.98	5181.12
303	279.61	276.64	252.97	26.64	709.69	23.67	560.27
403	285.56	283.58	286.47	-0.91	0.83	-2.89	8.35
503	289.52	284.81	306.21	-16.69	278.56	-21.4	457.96
603	292.25	288.78	318.6	-26.35	694.32	-29.82	889.23
703	293.98	290.02	327.2	-33.22	1103.57	-37.18	1382.35
803	295.96	291.5	333.3	-37.34	1394.28	-41.8	1747.24
903	296.96	292.25	337.8	-40.84	1667.91	-45.55	2074.80
				Sum	11102.50		12301.33
				MSE	1387.81	MSE	1537.67

Similarly, for the model calculating the effect of length on the clearance of Urea, Table 19 shows the value for MSE once the model is compared with the existing literature.

Table 19 Table showing Mean square error for model calculating clearance w.r.t hollow fiber length

Length of dialyzer fiber (cm)	Islam et al. Urea clearance rate (mL/min)	Tooba et al. Urea clearance rate (mL/min)	Model Predicted Urea clearance rate(mL/min)	Difference bw model and Tooba et al. clearance (Yi-Yi [^])	Difference bw model and Tooba et al. clearance squared	Difference bw model and Islam et al. clearance squared
27	243.89	247.23	289	-41.77	1744.7329	2034.9121
30	252.8	256.59	291.72	-35.13	1234.1169	1514.7664
33	260.16	264.17	293.75	-29.58	874.9764	1128.2881
36	266.62	270.64	295.27	-24.63	606.6369	820.8225
39	272.2	275.32	296.42	-21.1	445.21	586.6084
42	276.66	280.22	297.28	-17.06	291.0436	425.1844

45	280.89	283.57	297.93	-14.36	206.2096	290.3616
48	284.01	286.24	298.43	-12.19	148.5961	207.9364
51	285.57	288.69	298.8	-10.11	102.2121	175.0329
54	288.03	290.7	299.09	-8.39	70.3921	122.3236
Sum					5724.13	7306.24
MSE					572.41	730.62

Table 20 Table showing Mean square error for model calculating clearance w.r.t hollow fiber radius

The radius of hollow fibers (um)	Islam et al. Urea clearance rate (mL/min)	Tooba et al. Urea clearance rate (mL/min)	Model Predicted Urea clearance rate (mL/min)	Difference bw model and Tooba et al. clearanc e (Yi-Yi [^])	Difference bw model and Tooba et al. clearance squared	Difference bw model and Islam et al. clearance (Yi-Yi [^])	Difference bw model and Islam et al. clearance squared
100	243.9	248.49	288.64	-40.15	1612.0225	-44.74	2001.6676
110	249.55	253.6	291.18	-37.58	1412.2564	-41.63	1733.0569
120	255.2	258.45	293.14	-34.69	1203.3961	-37.94	1439.4436
130	258.42	263.02	294.65	-31.63	1000.4569	-36.23	1312.6129
140	262.46	266.51	295.82	-29.31	859.0761	-33.36	1112.8896
150	266.49	269.73	296.73	-27	729	-30.24	914.4576
160	268.63	272.14	297.44	-25.3	640.09	-28.81	830.0161
170	270.5	274.55	297.99	-23.44	549.4336	-27.49	755.7001
180	273.45	276.96	298.43	-21.47	460.9609	-24.98	624.0004
190	274.5	278.29	298.8	-20.51	420.6601	-24.3	590.49
200	277.46	279.89	299.06	-19.17	367.4889	-21.6	466.56
Sum					9254.84		11780.89
MSE					841.35	MSE	1070.99

The mean square error values higher than 0 indicate that the data points are dispersed at various points around the mean of data. Hence a lower MSE model is a better-fit model than the one with a higher MSE.

4.2.3 Coefficient of Determination

R squared, or the coefficient of determination represents the difference between the predicted and actual values. Its value varies between 0 and 1. 0 denotes that the model cannot explain any of the values in the dataset. In contrast, values closer to 1 depict that model can be used to describe the variation occurring in the values across various input values. Eq. (16) was used to find R^2 in which, Y_i' represents the model-predicted values, \bar{Y} represents the mean of actual values, Y_i represents the actual values, and n is the number of values in the dataset.

Table 21 Table showing R square values for the model predicting the clearance w.r.t dialysate flow rate

Dialysate flow rate (mL/min)	Tooba et al. clearance (mL/min)	Islam et al. clearance (mL/min)	Model predicted clearance (mL/min)	Difference bw model predicted and Tooba et al. clearance ($Y_i' - Y$)	Difference bw model predicted values and Tooba et al. predicted values squared	Difference bw model and mean value of Tooba et al. clearance ($Y_i - \bar{Y}$)
203	266.23	265.73	193.75	-72.48	5253.3504	-93.7588
303	279.61	276.64	252.97	-26.64	709.6896	-34.5388
403	285.56	283.58	286.47	0.91	0.8281	-1.03875
503	289.52	284.81	306.21	16.69	278.5561	18.70125
603	292.25	288.78	318.6	26.35	694.3225	31.09125
703	293.98	290.02	327.2	33.22	1103.5684	39.69125
803	295.96	291.5	333.3	37.34	1394.2756	45.79125
903	296.96	292.25	337.8	40.84	1667.9056	50.29125
				Sum	11102.50	

$$R^2=0.63$$

The general rule is that the more the value of R^2 is closer to 1, the better the model predicts the data, or it indicates that the difference between the observed and the predicted values is small.

4.3 Sensitivity Analysis

4.3.1 What is sensitivity analysis?

Sensitivity analysis is a technique used to evaluate the effect of one or two input parameters on the output parameter and is widely used in various fields worldwide. It is used to analyze how sensitive output is to the input. There are two types of sensitivity analysis commonly performed. The first one is the single variable sensitivity analysis, where there is a change in the value of a single variable while all other variables are kept constant. The second is two-variable sensitivity, where two variables are varied to find the effect on the output parameter [74, 75]. Sensitivity analysis considers mathematical models to predict the parameter outcome with certain input conditions. It addresses the what-if-the-key-inputs-or-assumptions-changed questions [76]. So, it can be described as a data-based forecast incorporating uncertainty into the decision-making process.

A two-variable sensitivity analysis is performed using MS Excel to find the effect of change in length and radius on clearance with changing dialysate flow rate values. For simplicity, five values of each variable are used, and the ‘What-if analysis’ function is used from the Data toolbar in Excel.

Table 22 Two variable sensitivity analysis showing a change in clearance with changing length and dialysate flow rates

		Length of hollow fiber (cm)				
275		21	22	23	24	25
Dialysate flow rate (mL/min)	800	287.69	289.23	290.58	291.75	292.78
	700	285.60	287.27	288.75	290.05	291.19
	600	282.37	284.21	285.85	287.32	288.63
	500	276.94	278.98	280.83	282.51	284.03
	400	266.68	268.91	270.96	272.84	274.58

Table 22 shows the effect of a change in Urea clearance value with a change in the length of hollow fibers and dialysate flow rates. The highlighted cell shows the value of clearance that we target. The table shows the clearance values in each cell, which is the combination of each top row and initial column. 275 mL/min is the operator

value or can also be stated as the reference value against which all rest of the values are calculated.

Table 23 Two variable sensitivity analysis showing a change in clearance with changing radius and dialysate flow rates

		Radius of hollow fiber (cm)					
		275	0.01	0.02	0.03	0.04	0.05
Dialysate flow rate (mL/min)	800	285.92	299.00	299.93	299.99	300.00	
	700	283.69	298.56	299.87	299.99	300.00	
	600	280.29	297.70	299.72	299.97	300.00	
	500	274.67	295.70	299.21	299.85	299.97	
	400	264.25	289.81	296.64	298.85	299.60	

Table 23 shows the effect of the change in the value of Urea clearance with the change in the radius of hollow fibers and dialysate flow rates. The highlighted cell shows the value of clearance that we target. The table shows the clearance values in each cell, which is the combination of each top row and initial column. The operator value (275 mL/min) is the reference value against which all the values are calculated.

Conclusion and Recommendations

Summary of Findings

The study aimed to develop a user-friendly app that enables people carrying out the hemodialysis process to track the prognosis of the disease conveniently and monitor the hemodialysis process. Initially, the effect of change in blood and dialysate flow on the clearance was observed, and it was found that the model for change in Urea clearance for blood flow rate was in relatively good agreement with experimental data because the percentage difference was <10% in both blood flow rate arrangements compared to previous in silico models. The model showing the change in Urea clearance with changing dialysate flow rate showed that initially, at lower dialysate flow rates, predicted clearance is 37% less than previous models. Increasing dialysate flow rates reduces this percentage difference, which ultimately comes to 13%. Change in Urea concentration with time model showed a drop in Urea concentration was initially more prominent. However, during the second half of the process, with the passage of each 25 minutes interval, the drop in Urea concentration is 1 mmol/L. When evaluating the effect of flow orientation, it was observed that at very high dialysate flow rates, the percentage difference in clearance value decreases, as it was found to be 16% at 1000 mL/min as compared to 31% at 400 mL/min which is its usual inception point. Comparison of Urea clearance with different K_oA showed that with an increase in value of K_oA of 300 mL/min, the percentage increase in Urea clearance was almost 12%. With increasing length and diameter of hollow fiber, it was found that model-predicted clearances had a high percentage difference with previous models initially. However, increasing the length and radius of hollow fibers reduces this percentage difference. Exploring the relationship between standard KT/V and reduced renal function showed that with increasing renal function by a value of 0.5 mL/min, there was twice an increase in the value of std KT/V . Also, by incrementing a single weekly session, the std KT/V value doubles.

Limitations and Future Research Directions

The accuracy of the user-friendly app can further be enhanced by incorporating a CFD model on the backend, which considers tortuosity, porosity, initial conditions and boundary conditions into consideration. It can result in increased accuracy, but it will

require more time to process, and a suitable processing machine will ultimately increase the cost of the app. Also, carrying out any changes in such an app would require a solid theoretical background in fluids. It would only allow engineers to carry out any changes in the backend code later. However, the challenge can be overcome by collaborating and carrying out interdisciplinary research and explorations, as it can familiarize developers and users with different app aspects and troubleshoot its issues. More research and explorations can be done toward developing such an efficient, cost-efficient, easy-to-use app.

References

- [1] T. Yaqoob, M. Ahsan, S. Farrukh, and I. Ahmad, "Design and Development of a Computational Tool for a Dialyzer by Using Computational Fluid Dynamic (CFD) Model," *Membranes (Basel)*, vol. 11, Nov 24 2021.
- [2] C. Theodorou, R. Leatherby, and R. Dhanda, "Function of the nephron and the formation of urine," *Anaesthesia & Intensive Care Medicine*, vol. 22, pp. 434-438, 2021.
- [3] T. Blanc, N. Goudin, M. Zaidan, M. G. Traore, F. Bienaime, L. Turinsky, *et al.*, "Three-dimensional architecture of nephrons in the normal and cystic kidney," *Kidney International*, vol. 99, pp. 632-645, 2021/03/01/ 2021.
- [4] S. Geurts, A. C. van der Burgh, M. M. Bos, M. A. Ikram, B. H. C. Stricker, J. W. Deckers, *et al.*, "Disentangling the association between kidney function and atrial fibrillation: a bidirectional Mendelian randomization study," *International Journal of Cardiology*, vol. 355, pp. 15-22, 2022/05/15/ 2022.
- [5] A. Levin, R. Agarwal, W. G. Herrington, H. L. Heerspink, J. F. E. Mann, S. Shahinfar, *et al.*, "International consensus definitions of clinical trial outcomes for kidney failure: 2020," *Kidney International*, vol. 98, pp. 849-859, 2020/10/01/ 2020.
- [6] P. P. Hsiue, T. Sekimura, A. Ocampo, C. J. Chen, T. E. Olson, B. V. Kelley, *et al.*, "Impact of renal disease on elective shoulder arthroplasty outcomes for glenohumeral osteoarthritis," *Seminars in Arthroplasty: JSES*, 2021/12/06/ 2021.
- [7] S. Valkenburg, G. Glorieux, and R. Vanholder, "Uremic Toxins and Cardiovascular System," *Cardiology Clinics*, vol. 39, pp. 307-318, 2021/08/01/ 2021.
- [8] S. Daneshamouz, U. Eduok, A. Abdelrasoul, and A. Shoker, "Protein-bound uremic toxins (PBUTs) in chronic kidney disease (CKD) patients: Production pathway, challenges and recent advances in renal PBUTs clearance," *NanoImpact*, vol. 21, p. 100299, 2021/01/01/ 2021.
- [9] H. Zhao, J. Huang, L. Miao, Y. Yang, Z. Xiao, Q. Chen, *et al.*, "Toward Urease-free wearable artificial kidney: Widened interlayer spacing MoS₂ nanosheets with

- highly effective adsorption for uremic toxins," *Chemical Engineering Journal*, vol. 438, p. 135583, 2022/06/15/ 2022.
- [10] J. C. Paz, "Genitourinary System," in *Acute Care Handbook for Physical Therapists*, ed, 2014, pp. 225-242.
- [11] O. Azhar, Z. Jahan, F. Sher, M. B. K. Niazi, S. J. Kakar, and M. Shahid, "Cellulose acetate-polyvinyl alcohol blend hemodialysis membranes integrated with dialysis performance and high biocompatibility," *Materials Science and Engineering: C*, vol. 126, p. 112127, 2021/07/01/ 2021.
- [12] N. Hala, M. Ariba, S. Sarush Ahmed, and S. Fahad Hassan, "Renal anarchy in Pakistan: Rising challenges for end-stage renal disease patients," *Ethics, Medicine and Public Health*, vol. 21, p. 100712, 2022/04/01/ 2022.
- [13] H. Wang, J. Ran, and T. Jiang, "Urea," *Subcell Biochem*, vol. 73, pp. 7-29, 2014.
- [14] M. Galach, A. Ciechanowska, S. Sabalińska, J. Waniewski, J. Wójcicki, and A. Weryńskis, "Impact of convective transport on dialyzer clearance," *Journal of artificial organs : the official journal of the Japanese Society for Artificial Organs*, vol. 6, pp. 42-8, 02/01 2003.
- [15] M. Faris and S. Al-Mukhtar, *Lecture 6 practical*, 2021.
- [16] G. Guerra, M. Lorenzini, M. Troncossi, and J. Farina, "Design and fluid dynamic analysis of a custom drip chamber in a medical disposable device," 2015.
- [17] A. T. Azar, "Dialyzer performance parameters," *Modelling and Control of Dialysis Systems: Volume 1: Modeling Techniques of Hemodialysis Systems*, pp. 379-425, 2013.
- [18] B. M. Robinson, T. Akizawa, K. J. Jager, P. G. Kerr, R. Saran, and R. L. Pisoni, "Factors affecting outcomes in patients reaching end-stage kidney disease worldwide: differences in access to renal replacement therapy, modality use, and haemodialysis practices."
- [19] I. K. Wang, C. L. Lin, T. H. Yen, S. Y. Lin, and F. C. Sung, "Comparison of survival between hemodialysis and peritoneal dialysis patients with end-stage renal disease in the era of icodextrin treatment," *Eur J Intern Med*, vol. 50, pp. 69-74, Apr 2018.

- [20] R. E. Patzer, M. Di, R. Zhang, L. McPherson, D. A. DuBay, M. Ellis, *et al.*, "Referral and Evaluation for Kidney Transplantation Following Implementation of the 2014 National Kidney Allocation System," *American Journal of Kidney Diseases*, 2022/03/14/ 2022.
- [21] P. Salamin, C. Deslarzes-Dubuis, A. Longchamp, S. Petitprez, J.-P. Venetz, J.-M. Corpataux, *et al.*, "Predictive Factors of Surgical Complications in the First Year Following Kidney Transplantation," *Annals of Vascular Surgery*, 2021/10/20/ 2021.
- [22] J. Portolés, A. Vega, E. Lacoba, P. López-Sánchez, M. Botella, C. Yuste, *et al.*, "Is peritoneal dialysis suitable technique CKD patients over 65 years? A prospective multicenter study," *Nefrología (English Edition)*, vol. 41, pp. 529-538, 2021/09/01/ 2021.
- [23] M. Suleman, M. Shadrack, D. Msuya, S. Chugulu, K. Chilonga, D. McHaile, *et al.*, "Foley catheter used for peritoneal dialysis," *Journal of Pediatric Surgery Case Reports*, vol. 75, p. 102085, 2021/12/01/ 2021.
- [24] Z.-Y. Guo, W.-J. Yuan, and W.-K. Lo, "Role of soluble intercellular adhesion molecule-1 in the process of peritonitis in peritoneal dialysis," *Hong Kong Journal of Nephrology*, vol. 4, pp. 87-89, 2002/10/01/ 2002.
- [25] D. L. Cull, "Role of Prosthetic Hemodialysis Access Following Introduction of the Dialysis Outcome Quality and Fistula First Breakthrough Initiatives," *Seminars in Vascular Surgery*, vol. 24, pp. 89-95, 2011/06/01/ 2011.
- [26] E. Nadort, N. Rijkers, R. W. Schouten, E. K. Hoogeveen, W. J. W. Bos, L. J. Vleming, *et al.*, "Depression, anxiety and quality of life of hemodialysis patients before and during the COVID-19 pandemic," *Journal of Psychosomatic Research*, p. 110917, 2022/04/14/ 2022.
- [27] M. Leung, W. Jung J Fau - Lau, M. Lau W Fau - Kiaii, B. Kiaii M Fau - Jung, and B. Jung, "Best possible medication history for hemodialysis patients obtained by a pharmacy technician."
- [28] R. Baker, "Membrane Technology And Applications," *Metallurgical Transactions A*, vol. 6, 05/01 2004.

- [29] M. V. Voinova, "Modeling water transport processes in dialysis," *arXiv: Tissues and Organs*, 2018.
- [30] S. Talluri and S. Lohani, "The Rise, Fall, and New Rise of Home Hemodialysis," *Kidney News*, vol. 13, pp. 20-20, 01 Sep. 2021 2021.
- [31] C. Ronco, "The Rise of Expanded Hemodialysis," *Blood Purification*, vol. 44, pp. I-VIII, 2017.
- [32] D. R. Ward, L. M. Moist, J. M. MacRae, N. Scott-Douglas, J. Zhang, M. Tonelli, *et al.*, "Risk factors associated with hemodialysis central venous catheter malfunction; a retrospective analysis of a randomized controlled trial," *Can J Kidney Health Dis*, vol. 1, p. 15, 2014.
- [33] J. G. Speight, *Chemical Process and Design Handbook*, 1st Edition ed. New York: McGraw-Hill Education, 2002.
- [34] N. Ferraz, A. Leschinskaya, F. Toomadj, B. Fellström, M. Strømme, and A. Mhraryan, "Membrane characterization and solute diffusion in porous composite nanocellulose membranes for hemodialysis," *Cellulose*, vol. 20, pp. 2959-2970, 2013/12/01 2013.
- [35] M. Karsten, S. George, and T. Florian, "The derivation of the linear Boltzmann equation from a Rayleigh gas particle model," *Kinetic and Related Models*, vol. 11IS - 2SP - 1, p. 41, 2018.
- [36] C. Ronco, N. Marchionna, A. Brendolan, M. Neri, A. Lorenzin, and A. J. Martínez Rueda, "Expanded haemodialysis: from operational mechanism to clinical results."
- [37] M. Ali, Z. Jahan, F. Sher, M. B. Khan Niazi, S. J. Kakar, and S. Gul, "Nano architected cues as sustainable membranes for ultrafiltration in blood hemodialysis," *Materials Science and Engineering: C*, vol. 128, p. 112260, 2021/09/01/ 2021.
- [38] L. Kahlenberg, "On the Nature of the Process of Osmosis and Osmotic Pressure with Observations Concerning Dialysis," *The Journal of Physical Chemistry*, vol. 10, pp. 141-209, 1906/03/01 1906.
- [39] N. J. Ofsthun and J. K. Leypoldt, "Ultrafiltration and backfiltration during hemodialysis."

- [40] C. S. C. Bouman, R. W. van Olden, and C. P. Stoutenbeek, "Cytokine Filtration and Adsorption during Pre- and Postdilution Hemofiltration in Four Different Membranes," *Blood Purification*, vol. 16, pp. 261-268, 1998.
- [41] P. Valette, M. Thomas, and P. Déjardin, "Adsorption of low molecular weight proteins to hemodialysis membranes: experimental results and simulations," *Biomaterials*, vol. 20, pp. 1621-1634, 1999/09/01/ 1999.
- [42] P. J. Soltys, A. Zydney, J. K. Leypoldt, L. W. Henderson, and N. J. Ofsthun, "Potential of dual-skinned, high-flux membranes to reduce backtransport in hemodialysis," *Kidney International*, vol. 58, pp. 818-828, 2000/08/01/ 2000.
- [43] H. Morel, "Acid-base balance in online hemodiafiltration: modeling, in vitro and in vivo analyses of bicarbonate transfers

Equilibre acide-base lors de l'hémodiafiltration en ligne : modélisation, analyses in vitro et clinique des transferts de bicarbonate," Université de Technologie de Compiègne, 2009.

- [44] C. Legallais, G. Catapano, B. Von Harten, and U. Baurmeister, "A theoretical model to predict the in vitro performance of hemodiafilters," *Journal of Membrane Science*, vol. 168, pp. 3-15, 04/15 2000.
- [45] L. Coli, A. Ursino M Fau - De Pascalis, C. De Pascalis A Fau - Brighenti, V. Brighenti C Fau - Dalmastrì, G. Dalmastrì V Fau - La Manna, E. La Manna G Fau - Isola, *et al.*, "Evaluation of intradialytic solute and fluid kinetics. Setting Up a predictive mathematical model."
- [46] M. Galach, A. Ciechanowska, S. Sabalińska, J. Waniewski, J. M. Wojcicki, and A. Weryńskis, "Impact of convective transport on dialyzer clearance," *Journal of Artificial Organs*, vol. 6, pp. 0042-0048, 2003.
- [47] M. Y. Jaffrin, J. M. Ding Lh Fau - Laurent, and J. M. Laurent, "Simultaneous convective and diffusive mass transfers in a hemodialyser."
- [48] S. A. Conrad and A. Bidani, "Finite element mathematical model of fluid and solute transport in hemofiltration membranes," in *Proceedings of the 25th Annual International Conference of the IEEE Engineering in Medicine and Biology Society (IEEE Cat. No.03CH37439)*, 2003, pp. 423-426 Vol.1.

- [49] Z. Mimouni, "The Rheological Behavior of Human Blood—Comparison of Two Models," *Open Journal of Biophysics*, vol. 06, pp. 29-33, 01/01 2016.
- [50] M. Gałach and A. Weryński, "Development of "virtual patient" model for simulation of solute and fluid transport during dialysis," *Bulletin of the Polish Academy of Sciences Technical Sciences*, vol. vol. 53, pp. 283-292, 2005 2005.
- [51] K.-i. Yamamoto, M. Hayama, M. Matsuda, T. Yakushiji, M. Fukuda, T. Miyasaka, *et al.*, "Evaluation of asymmetrical structure dialysis membrane by tortuous capillary pore diffusion model," *Journal of Membrane Science*, vol. 287, pp. 88-93, 2007/01/05/ 2007.
- [52] A. T. Azar, "Increasing dialysate flow rate increases dialyzer urea clearance and dialysis efficiency: an in vivo study."
- [53] J. C. Olson, "Design and modeling of a portable hemodialysis system," 2009.
- [54] A. Hedayat, J. Szpunar, N. A. P. K. Kumar, R. Peace, H. Elmoselhi, and A. Shoker, "Morphological Characterization of the Polyflux 210H Hemodialysis Filter Pores," *International Journal of Nephrology*, vol. 2012, p. 304135, 2012/11/06 2012.
- [55] M. Islam and J. Szpunar, "Study of Dialyzer Membrane (Polyflux 210H) and Effects of Different Parameters on Dialysis Performance," *Open Journal of Nephrology*, vol. 03, pp. 161-167, 01/01 2013.
- [56] W. A.-O. Ding, W. Li, S. Sun, X. Zhou, P. A. Hardy, S. Ahmad, *et al.*, "Three-dimensional simulation of mass transfer in artificial kidneys."
- [57] E. Ravagli, E. Grandi, P. Rovatti, and S. Severi, "Finite-Element Modeling of Time-Dependent Sodium Exchange across the Hollow Fiber of a Hemodialyzer by Coupling with a Blood Pool Model," *The International Journal of Artificial Organs*, vol. 39, pp. 471-478, 2016/09/01 2016.
- [58] D. Donato, A. Boschetti-de-Fierro, C. Zweigart, M. Kolb, S. Eloit, M. Storr, *et al.*, "Optimization of dialyzer design to maximize solute removal with a two-dimensional transport model," *Journal of Membrane Science*, vol. 541, pp. 519-528, 2017/11/01/ 2017.
- [59] H. Wang, T. Ran J Fau - Jiang, and T. Jiang, "Urea."

- [60] I. Baldwin, M. Baldwin, N. Fealy, M. Neri, F. Garzotto, J. C. Kim, *et al.*, "Con-Current versus Counter-Current Dialysate Flow during CVVHD. A Comparative Study for Creatinine and Urea Removal," *Blood Purif*, vol. 41, pp. 171-6, 2016.
- [61] C. Ronco and D. Cruz, "Hemodialysis - From Basic Research to Clinical Trials," 2008.
- [62] E. M. Fazl, S. Ahmad, I. Elahi, and M. Anees, "Comparison between different methods of calculating Kt/V as the marker of adequacy of dialysis," *Pak J Med Sci*, vol. 38, pp. 167-171, Jan-Feb 2022.
- [63] K. Sennfalt, P. Magnusson M Fau - Carlsson, and P. Carlsson, "Comparison of hemodialysis and peritoneal dialysis--a cost-utility analysis."
- [64] M. Ziolk, J. A. Pietrzyk, and J. Grabska-Chrzastowska, "Accuracy of hemodialysis modeling," *Kidney Int*, vol. 57, pp. 1152-63, Mar 2000.
- [65] W. R. Clark and D. Gao, "Properties of membranes used for hemodialysis therapy," in *Seminars in Dialysis*, 2002, pp. 191-195.
- [66] T. Yaqoob, M. Ahsan, A. Hussain, and I. Ahmad, "Computational Fluid Dynamics (CFD) Modeling and Simulation of Flow Regulatory Mechanism in Artificial Kidney Using Finite Element Method," *Membranes (Basel)*, vol. 10, Jul 3 2020.
- [67] D. R. Hassell, F. M. van der Sande, J. P. Kooman, J. P. Tordoir, and K. M. Leunissen, "Optimizing dialysis dose by increasing blood flow rate in patients with reduced vascular-access flow rate," *Am J Kidney Dis*, vol. 38, pp. 948-55, Nov 2001.
- [68] W. E. Bloembergen, D. C. Stannard, F. K. Port, R. A. Wolfe, J. A. Pugh, C. A. Jones, *et al.*, "Relationship of dose of hemodialysis and cause-specific mortality," *Kidney Int*, vol. 50, pp. 557-65, Aug 1996.
- [69] J. K. Leypoldt, A. K. Cheung, L. Y. Agodoa, J. T. Daugirdas, T. Greene, P. R. Keshaviah, *et al.*, "Hemodialyzer mass transfer-area coefficients for urea increase at high dialysate flow rates," *Kidney International*, vol. 51, pp. 2013-2017, 1997/06/01/ 1997.
- [70] R. P. Babb Al Fau - Popovich, T. G. Popovich Rp Fau - Christopher, B. H. Christopher Tg Fau - Scribner, and B. H. Scribner, "The genesis of the square meter-hour hypothesis."

- [71] F. Gastaldon, A. Brendolan, C. Crepaldi, P. Frisone, S. Zamboni, V. D'Intini, *et al.*, "Effects of Novel Manufacturing Technology on Blood and Dialysate Flow Distribution in a New Low Flux "α Polysulfone" Hemodialyzer," *The International Journal of Artificial Organs*, vol. 26, pp. 105-112, 2003.
- [72] B. Saran R Fau - Robinson, K. C. Robinson B Fau - Abbott, L. Y. C. Abbott Kc Fau - Agodoa, P. Agodoa Ly Fau - Albertus, J. Albertus P Fau - Ayanian, R. Ayanian J Fau - Balkrishnan, *et al.*, "US Renal Data System 2016 Annual Data Report: Epidemiology of Kidney Disease in the United States," 2017.
- [73] T. Shafi and A. S. Levey, "Measurement and Estimation of Residual Kidney Function in Patients on Dialysis," *Adv Chronic Kidney Dis*, vol. 25, pp. 93-104, Jan 2018.
- [74] T. Lenhart, K. Eckhardt, N. Fohrer, and H. G. Frede, "Comparison of two different approaches of sensitivity analysis," *Physics and Chemistry of the Earth, Parts A/B/C*, vol. 27, pp. 645-654, 2002/01/01/ 2002.
- [75] F. Pianosi, F. Sarrazin, and T. Wagener, "A Matlab toolbox for Global Sensitivity Analysis," *Environmental Modelling & Software*, vol. 70, pp. 80-85, 2015/08/01/ 2015.
- [76] L. Thabane, L. Mbuagbaw, S. Zhang, Z. Samaan, M. Marcucci, C. Ye, *et al.*, "A tutorial on sensitivity analyses in clinical trials: the what, why, when and how," *BMC Medical Research Methodology*, vol. 13, p. 92, 2013/07/16 2013.